Inorg. Chem. **2005**, *44*, 4679–4692

Synthesis and Characterization of New Coordination Polymers Generated from Bent Bis(Cyanophenyl)oxadiazole Ligands and Ag(I) Salts

Yu-Bin Dong,* Hai-Ying Wang, Jian-Ping Ma, Da-Zhong Shen, and Ru-Qi Huang

College of Chemistry, Chemical Engineering and Materials Science, and Shandong Key Lab of Chemical Functional Materials, Shandong Normal University, Jinan 250014, People's Republic of China

Received February 10, 2005

Two new bent bis(cyanophenyl)oxadiazole ligands, 2,5-bis(4-cyanophenyl)-1,3,4-oxadiazole (**L7**) and 2,5-bis(3-cyanophenyl)-1,3,4-oxadiazole (**L8**), were synthesized. The coordination chemistry of these ligands with various Ag(I) salts has been investigated. Seven new coordination polymers, namely, $\{[Ag(\mathbf{L7})(H_2O)]ClO_4\}_n$ (**1**) (triclinic, $P\bar{1}$, $a = 9.342(4)$ Å, $b = 9.889(4)$ Å, $c = 10.512(4)$ Å, $\alpha = 68.978(6)°$, $\beta = 78.217(6)°$, $\gamma = 81.851(7)°$, $Z = 2$), $\{[Ag(\mathbf{L7})]SO_3CF_3\}_n$ (**2**) (monoclinic, $P2_1/n$, $a = 7.559(2)$ Å, $b = 23.739(6)$ Å, $c = 10.426(3)$ Å, $\beta = 108.071(4)°$, $Z = 4$), $\{[Ag(\mathbf{L8})]BF_4 \cdot 0.5(C_6H_6) \cdot H_2O\}_n$(**3**) (triclinic, $P\bar{1}$, $a = 7.498(3)$ Å, $b = 10.649(4)$ Å, $c = 13.673(5)$ Å, $\alpha = 98.602(5)°$, $\beta = 100.004(5)°$, $\gamma = 110.232(5)°$, $Z = 2$), $\{[Ag(\mathbf{L8})SbF_6] \cdot H_2O\}_n$ (**4**) (triclinic, $P\bar{1}$, $a = 8.2621(9)$ Å, $b = 10.6127(12)$ Å, $c = 13.3685(15)$ Å, $\alpha = 98.012(2)°$, $\beta = 106.259(2)°$, $\gamma = 112.362(2)°$, $Z = 2$), $\{[Ag_2(\mathbf{L8})_2(SO_3CF_3)] \cdot H_2O\}_n$ (**5**) (triclinic, $P\bar{1}$, $a = 10.713(4)$ Å, $b = 13.449(5)$ Å, $c = 15.423(5)$ Å, $\alpha = 65.908(5)°$, $\beta = 74.231(5)°$, $\gamma = 83.255(5)°$, $Z = 2$), $\{[Ag_2(\mathbf{L8})(C_6H_6)(ClO_4)] \cdot ClO_4\}_n$ (**6**) (monoclinic, $P2_1/n$, $a = 6.9681(17)$ Å, $b = 20.627(5)$ Å, $c = 17.437(4)$ Å, $\beta = 95.880(4)°$, $Z = 4$), and $\{[Ag_2(\mathbf{L8})(H_2PO_4)_2]\}_n$ (**7**) (triclinic, $P\bar{1}$, $a = 7.956(2)$ Å, $b = 9.938(3)$ Å, $c = 14.242(4)$ Å, $\alpha = 106.191(4)°$, $\beta = 97.322(4)°$, $\gamma = 107.392(4)°$, $Z = 1$), were obtained by the combination of **L7** and **L8** with Ag(I) salts in a benzene/methylene chloride mixed-solvent system and fully characterized by infrared spectroscopy, elemental analysis, and single-crystal X-ray diffraction. In addition, the luminescence and electrical conductance properties of compounds **1**–**6** and the host–guest chemistry of compound **3** were investigated.

Introduction

Within the field now called "inorganic/organic coordination polymers", efforts to use transition metal ions and organic spacers simultaneously have recently been extremely fruitful.[1−3] During the past decades, a number of these compounds, with interesting polymeric motifs, have been successfully designed and synthesized. Some of them exhibit encouraging potential for application in catalysis, nonlinear optics, gas separation, magnetic properties, and molecular recognition.[4] In general, primary control over the type and topology of the product generated from the self-assembly of inorganic metal codes and organic spacers can be achieved by the functionality of the ligand[5] and metal coordination

* To whom correspondence should be addressed. E-mail: yubindong@sdnu.edu.cn.

(1) Zaworotko, M. J.; Moulton, B. *Chem. Rev.* **2001**, *101*, 2619. (b) Eddaoudi, M.; Moler, D. B.; Li, H.; Chen, B.; Reineke, T. M.; Keeffe, M. O.; Yaghi, O. M. *Acc. Chem. Res.* **2001**, *34*, 319. (c) Constable, E. C. *Prog. Inorg. Chem*. **1994**, *42*, 67. (d) Hirsch, K. A.; Wilson, S. R.; Moore, J. S. *Inorg. Chem.* **1997**, *36*, 2960. (e) Dunbar, K. R.; Heintz, K. R. *Prog. Inorg. Chem*. **1996**, 283. (f) Whiteford, J. A.; Rachlin, E. M.; Stang, P. J. *Angew. Chem., Int. Ed. Engl*. **1996**, *35*, 2524. (g) Gardner, G. B.; Venkataraman, D.; Moore, J. S.; Lee, S. *Nature* **1995**, *374*, 792.

(2) Yaghi, O. M.; Li, G.; Li, H. *Nature* **1995**, *378*, 703. (b) Yaghi, O. M.; Li, H. *J. Am. Chem. Soc.* **1995**, *117*, 10401. (c) Yaghi, O. M.; Li, H.; Groy, T. L. *J. Am. Chem. Soc.* **1996**, *118*, 9096. (d) Fujita, M.; Oka, H.; Yamaguchi, K.; Ogura, K. *Nature* **1995**, *378*, 469. (e) Fujita, M.; Kwon, Y. J.; Sasaki, O.; Yamaguchi, K.; Ogura, K. *J. Am. Chem. Soc*. **1995**, *117*, 7287. (f) Losier, P.; Zaworotko, M. J. *Angew. Chem., Int. Ed. Engl*. **1996**, *35*, 2779. (g) Power, K. N.; Hennigar, T. L.; Zaworotko, M. J. *Chem. Commun*. **1998**, 595.

(3) Heintz, R. A.; Zhao, H.; Ouyang, X.; Grandinetti, G.; Cowen, J.; Dunbar, K. R. *Inorg. Chem.* **1999**, *38*, 144. (b) Mayr, A.; Guo, J. *Inorg. Chem*. **1999**, *38*, 921. (c) Su, C.-Y.; Goforth, A. M.; Smith, M. D.; Pellechia, P. J.; zur Loye, H.-C. *J. Am. Chem. Soc*. **2004**, *126*, 3576. (d) Mao, L. F.; Mayr, A. *Inorg. Chem*. **1996**, *35*, 3183. (e) Choi, H. J.; Suh, M. P. *J. Am. Chem. Soc.* **1998**, *120*, 10622. (f) Sharma, C. V. K.; Broker, G. A.; Huddleston, J. G.; Baldwin, J. W.; Metzger, R. M.; Rogers, R. D. *J. Am. Chem. Soc*. **1999**, *121*, 1137.

10.1021/ic050218s CCC: $30.25
Published on Web 06/01/2005

geometry preference. For example, the combination of a linear rigid ligand, such as 4,4′-bipyridine or its derivatives, and a tetrahedral metal node will generate a diamondoid motif. In addition, the topology of the polymeric complexes can also be modified by the inorganic counterion,[6] solvent system,[6] and metal salt-to-ligand ratio,[7] which is demonstrated well by many previous studies. It is well-known that the rigid linear ligands have been the main theme in the chemistry of coordination polymers and have proven to be among the most important types of organic ligands for the design and construction of coordination polymers exhibiting remarkable polymeric structural motifs.[8] However, until now, little attention has been paid to the organic−inorganic coordination polymers or supramolecular complexes generated from bent organic ligands. Compared to rigid linear organic ligands, the bent rigid organic spacers do not propagate the metal coordination code legibly into the metal−organic architectures which makes it more difficult to forecast the coordination network topologies. Thus, the coordination chemistry of complexes based on bent organic ligands is more attractive.

Our research group has investigated the construction of coordination polymers and supramolecular complexes with the bent organic ligands. As shown in Scheme 1, in this project, five-membered oxadiazole and triazole heteroatom cyclic rings were chosen as the bridge, pyridyl, and aminophenyl groups of the terminal coordination sites (**L1**−**L6**).[9] As a result of the specific geometry of five-membered heterocycle-bridging ligands and the coordination preferences

Scheme 1. Bent Organic Ligands Used in the Construction of Coordination Polymers and Supramolecular Complexes

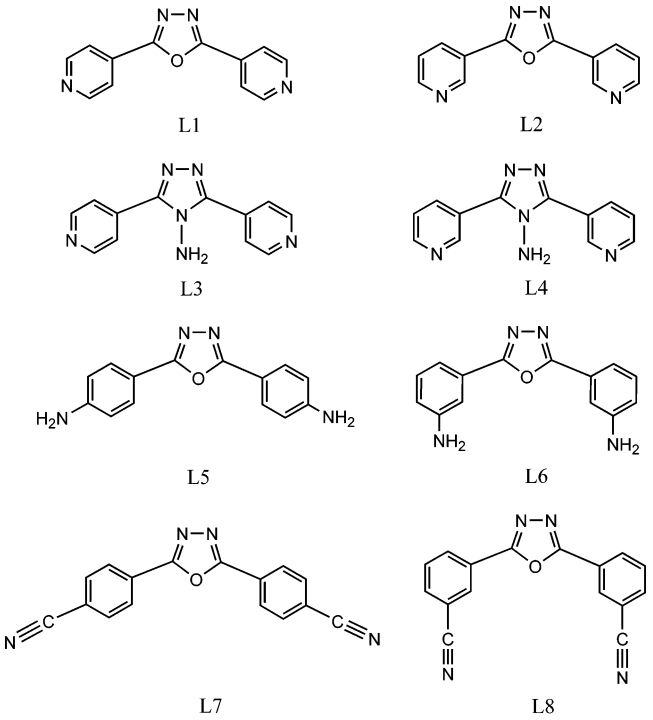

of the transition metals, various new types of coordination polymers, some with open channels and interesting luminescent properties, have been obtained. This encourages us to continue this project and expand the symmetric five-membered heterocycle-bridging bipyridine and biphenylamine types of ligands to include symmetric five-membered heterocycle-bridged bibenzonitrile ligands **L7** and **L8** (Scheme 2). Herein, we wish to report seven new Ag(I)-containing coordination polymers with novel polymeric motifs, namely, $\{[Ag(\mathbf{L7})(H_2O)]ClO_4\}_n$ (**1**), $\{[Ag(\mathbf{L7})]SO_3CF_3\}_n$ (**2**), $\{[Ag(\mathbf{L8})]BF_4 \cdot 0.5(C_6H_6) \cdot H_2O\}_n$ (**3**), $\{[Ag(\mathbf{L8})SbF_6] \cdot H_2O\}_n$ (**4**), $\{[Ag_2(\mathbf{L8})_2(SO_3CF_3)] \cdot H_2O\}_n$ (**5**), $\{[Ag_2(\mathbf{L8})(C_6H_6)(ClO_4)] \cdot ClO_4\}_n$ (**6**), and $\{[Ag_2(\mathbf{L8})(H_2PO_4)_2]\}_n$ (**7**), generated from **L7** and **L8** (Scheme 2) and various Ag(I) salts in solution.

Experimental Section

Materials and Methods. $AgSO_3CF_3$, $AgClO_4$, $AgPF_6$, $AgBF_4$, $AgSbF_6$, and AgH_2PO_4 (Acros) were used as obtained without further purification. Infrared (IR) samples were prepared as KBr

(4) Kobel, W.; Hanack, M. *Inorg. Chem.* **1986**, *25*, 103. (b) Kato, R.; Kobayashi, H.; Kobayashi, A. *J. Am. Chem. Soc.* **1989**, *111*, 5224. (c) Sinzger, K.; Hünig, S.; Jopp, M.; Bauer, D.; Bietsch, W.; von Schütz, J. U.; Wolf, H. C.; Kremer, R. K.; Metzenthin, T.; Bau, R.; Khan, S. I.; Lindaum, A.; Lengauer, C. L.; Tillmanns, E. *J. Am. Chem. Soc.* **1993**, *115*, 7696. (d) Erk, P.; Gross, H.-J.; Hünig, U. L.; Meixner, H.; Werner, H.-P.; von Schütz, J. U.; Wolf, H. C. *Angew. Chem., Int. Ed. Engl.* **1989**, *28*, 1245. (e) Jung, O.; Pierpont, C. G. *J. Am. Chem. Soc.* **1994**, *116*, 2229. (f) Patoux, C.; Loudret, C.; Launay, L. P.; Joachim, C.; Gourdon, A. *Inorg. Chem.* **1997**, *36*, 5037. (g) Dybtsev, D. N.; Chun, H.; Yoon, S. H.; Kim, D.; Kim, K. *J. Am. Chem. Soc.* **2004**, *126*, 32. (h) Maji, T. K.; Uemura, K.; Chang, H.-C.; Matsuda, R.; Kitagawa, S. *J. Am. Chem. Soc.* **2004**, *126*, 3269.

(5) Kuroda-Sowa, T.; Horrino, T.; Yamamoto, M.; Ohno, Y.; Maekawa, M.; Munakata, M. *Inorg. Chem.* **1997**, *36*, 6382. (b) Munakata, M.; Wu, L. P.; Kuroda-Sowa, T. *Bull. Chem. Soc. Jpn.* **1997**, *70*, 1727. (c) Munakata, M.; Wu, L. P.; Kuroda-Sowa, T.; Maekawa, M.; Moriwaki, K.; Kitagawa, S. *Inorg. Chem.* **1997**, *36*, 5416. (d) Hennigar, T. L.; MacQuarrie, D. C.; Losier, P.; Rogers, R. D.; Zaworotko, M. J. *Angew. Chem., Int. Ed. Engl.* **1997**, *36*, 972.

(6) Lu, J.; Paliwala, T.; Lim, S. C.; Yu, C.; Niu, T.; Jacobson, A. J. *Inorg. Chem.* **1997**, *36*, 923. (b) Munakata, M.; Ning, G. L.; Kuroda-Sowa, T.; Maekawa, M.; Suenaga, Y.; Harino, T. *Inorg. Chem.* **1998**, *37*, 5651. (c) Power, K. N.; Hennigar, T. L.; Zaworotko, M. J. *New J. Chem.* **1998**, *22*, 177. (d) Jung, O. S.; Park, S. H.; Kim, K. M.; Jang, H. G. *Inorg. Chem.* **1998**, *37*, 5781.

(7) Gable, R. W.; Hoskins, B. F.; Robson, R. *J. Chem. Soc., Chem. Commun.* **1990**, 1677. (b) Fujita, M.; Kwon, Y. J.; Washizu, S.; Ogura, K. *J. Am. Chem. Soc.* **1994**, *116*, 1151. (c) Robson, R.; Abrahams, B. F.; Batten, S. R.; Gable, R. W.; Hoskins, B. F.; Liu, J. In *Supramolecular Architecture*; Bein, T., Ed.; ACS Symposium Series 449; American Chemical Society: Washington, DC, 1992; Chapter 19. (d) Carlucci, L.; Ciani, G.; Proserpio, D. M.; Sironi, A. *J. Chem. Soc., Chem. Commun.* **1994**, 2755.

(8) Hagrman, P. J.; Hagrman, D.; Zubieta, J. *Angew. Chem., Int. Ed.* **1999**, *38*, 2638. (b) Blake, A. J.; Champness, N. R.; Hubberstey, P.; Li, W.-S.; Withersby, M. A.; Schröder, M. *Coord. Chem. Rev.* **1999**, *183*, 117. (c) Batten, S.; Robson, R. *Angew. Chem., Int. Ed.* **1998**, *37*, 1460. (d) Barnett, S. A.; Champness, N. R. *Coord. Chem. Rev.* **2003**, *246*, 145.

(9) (a) Dong, Y.-B.; Ma, J.-P.; Smith, M. D.; Huang, R.-Q.; Tang, B.; Chen, D.; zur Loye, H.-C. *Solid State Sci.* **2002**, *4*, 1313. (b) Dong, Y.-B.; Ma, J.-P.; Huang, R.-Q.; Smith, M. D.; zur Loye, H.-C. *Inorg. Chem.* **2003**, *42*, 294. (c) Dong, Y.-B.; Ma, J.-P.; Smith, M. D.; Huang, R.-Q.; Tang, B.; Guo, D.-S.; Wang, J.-S.; zur Loye, H.-C. *Solid State Sci.* **2003**, *5*, 601. (d) Dong, Y.-B.; Ma, J.-P.; Smith, M. D.; Huang, R.-Q.; Wang, J.-S.; zur Loye, H.-C. *Solid State Sci.* **2003**, *5*, 1177. (e) Dong, Y.-B.; Cheng, J.-Y.; Wang, H.-Y.; Huang, R.-Q.; Tang, B.; Smith, M. D.; zur Loye, H.-C. *Chem. Mater.* **2003**, *15*, 2593. (f) Dong, Y.-B.; Ma, J.-P.; Huang, R.-Q.; Liang, F.-Z.; Smith, M. D. *J. Chem. Soc., Dalton Trans.* **2003**, *9*, 1472. (g) Dong, Y.-B.; Cheng, J.-Y.; Huang, R.-Q.; Tang, B.; Smith, M. D.; zur Loye, H.-C. *Inorg. Chem.* **2003**, *42*, 5699. (h) Cheng, J.-Y.; Dong, Y.-B.; Ma, J.-P.; Huang, R.-Q.; Smith, M. D. *Inorg. Chem. Commun.* **2005**, *8*, 6. (i) Dong, Y.-B.; Cheng, J.-Y.; Huang, R.-Q.; Smith, M. D. *Inorg. Chim. Acta* **2005**, *385*, 901. (j) Dong, Y.-B.; Cheng, J.-Y.; Ma, J.-P.; Huang R.-Q.; Smith, M. D. *Crystal Growth & Design* **2005**, *5*, 585. (k) Dong, Y.-B.; Wang, H.-Y.; Ma, J.-P.; Huang, R.-Q.; Smith, M. D. *Cryst. Growth Des.* **2005**, *359*, 891.

Scheme 2. Synthesis of Ligands **L7** and **L8**

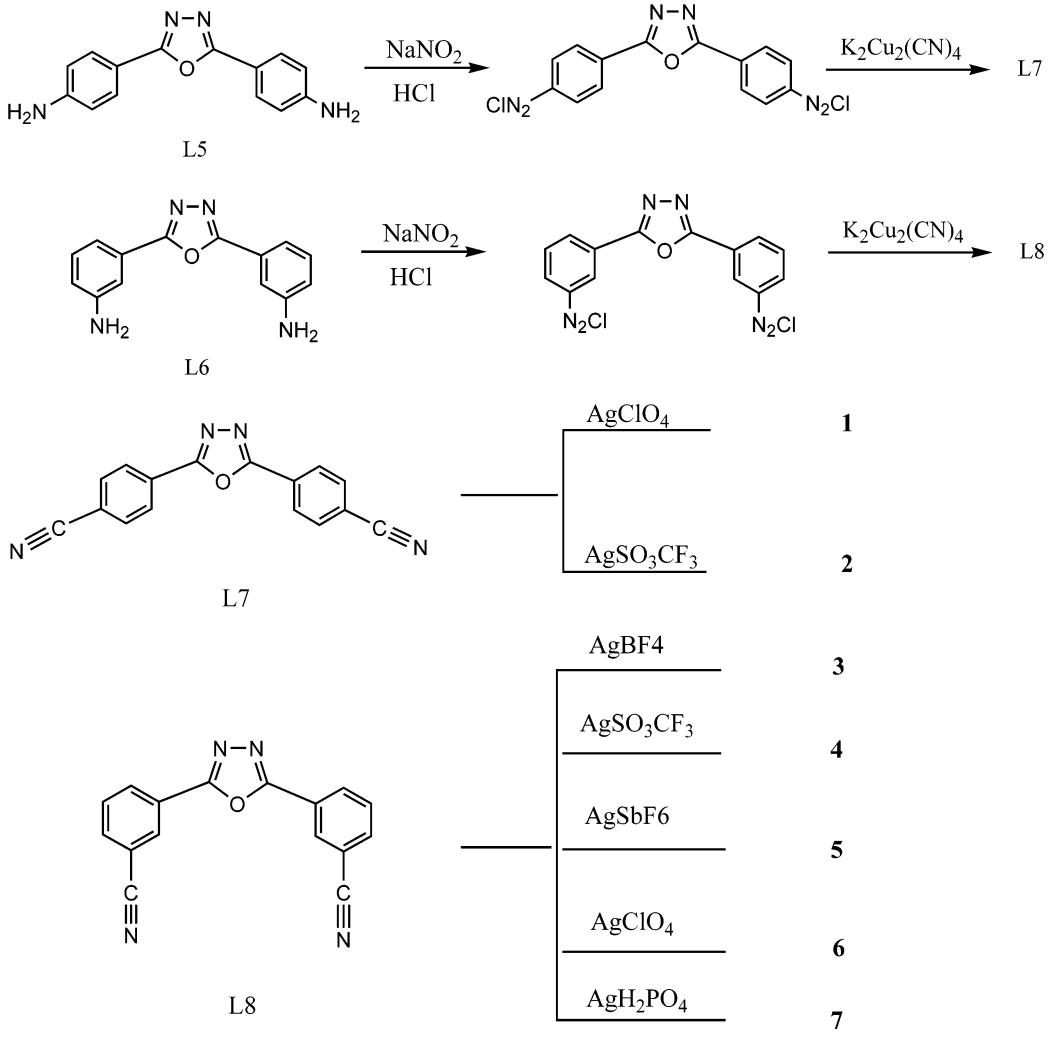

pellets, and the spectra were obtained in the 400−4000 cm^{-1} range using a Perkin-Elmer 1600 FTIR spectrometer. Elemental analyses were performed on a Perkin-Elmer Model 2400 analyzer. ^1H NMR data were collected using an AM-300 spectrometer. Chemical shifts are reported in δ relative to TMS. All fluorescence measurements were carried out on a Cary Eclipse spectrofluorimeter (Varian, Australia) equipped with a xenon lamp and quartz carrier at room temperature. Thermogravimetric analyses were carried out using a TA instrument SDT 2960 simultaneous DTA-TGA under flowing nitrogen at a heating rate of 10 °C/min. XRD patterns were obtained on a Rigaku D/Max-rB X-ray powder diffraction (XRD) apparatus with Cu Kα radiation (λ=1.5405 & Aring). Electrical conductivity was performed on an Agilent Technologies model 4294A-ATO-20150 instrument. *Caution! Two of the crystallization procedures involve $AgClO_4$ which is a strong oxidizer.*

Preparation of L7 and L8. An aqueous solution of $NaNO_2$ (1.50 g, 22 mmol) was added to a solution of **L5** (1.26 g, 5 mmol) in concentrated hydrochloric acid (25 mL) at 0 °C. The mixture was stirred for 1 h at room temperature. The diazonium salt solution, washed with 10% aqueous $NaHCO_3$, was added to an aqueous solution of $K_2Cu_2(CN)_4$, generated from the reaction of $CuSO_4 \cdot 5H_2O$ (2.6 g, 1.04 mmol), $NaHSO_3$ (0.56 g, 5.4 mmol) and KCN (2.64 g, 41 mmol). The mixture was stirred at room temperature overnight, and then the temperature was gradually increased to 80 °C; then, the mixture was stirred for 0.5 h. The mixture was allowed to cool to room temperature, and the product was collected by vacuum filtration and dried in air. The product was purified by column chromatrography on silica gel using CH_2Cl_2 as an eluent to produce **L7** (0.35 g) as a light yellow solid (26% yield). ^1H NMR (DMSO): δ 8.35−8.33 (d, 4H, C_6H_4), 8.13−8.10 (d, 4H, C_6H_4). IR (KBr): 2230 (s), 1653 (s), 1572 (s), 1539 (s), 1485 (s), 1411 (s), 1312 (s), 1274 (m), 1098 (s), 1060 (s), 1014 (s), 960 (s), 863 (s), 742 (s), 700 (s), 586 (s), 547 (s) cm^{-1}. Anal. Calcd for $C_{16}H_8N_4O$ (**L7**): C, 70.59; H, 2.94; N, 20.59. Found: C, 70.41; H, 2.80; N, 20.34. UV−vis spectrum (in CH_3CN at room temperature): λ_{max} 297 nm.

L8 was prepared following the procedure described for **L7** except **L6** was used instead of **L5** to produce **L8** in a 28% yield as a light pink crystalline solid. ^1H NMR (DMSO): δ 8.67 (s, 2H, C_6H_4), 8.50−8.48 (d, 2H, C_6H_4), 8.14−8.12 (d, 2H, C_6H_4), 7.88−7.83 (t, 2H, C_6H_4). IR (KBr): 2234 (s), 1612 (s), 1548 (s), 1487 (s), 1408 (s), 1295 (s), 1187 (m), 1081 (s), 986 (m), 916 (m), 832 (s), 736 (s), 678 (s), 582 (s), 459 (m) cm^{-1}. Anal. Calcd for $C_{16}H_8N_4O$ (**L7**): C, 70.59; H, 2.94; N, 20.59. Found: C, 70.46; H, 2.82; N, 20.39. UV−vis spectrum (in CH_3CN at room temperature): λ_{max} 234 nm, 279 nm.

Preparation of $\{[Ag(L7)(H_2O)]ClO_4\}_n$ (1). A solution of $AgClO_4$ (12 mg, 0.052 mmol) in benzene (10 mL) was layered onto a solution of **L7** (9.0 mg, 0.033 mmol) in CH_2Cl_2 (10 mL). The solutions were left at room temperature for about 2 days, and colorless crystals were obtained. Yield: 54%. IR (KBr): 3463 (br), 2232 (s), 1650 (m), 1543 (s), 1490 (s), 1401 (s), 1274 (s), 1117

Table 1. Crystallographic Data for **L7** and **1**−**3**

	L7	1	2	3
empirical formula	$C_{16}H_8N_4O$	$C_{16}H_{10}AgClN_4O_6$	$C_{17}H_8AgF_3N_4O_4S$	$C_{19}H_{13}AgBF_4N_4O_2$
fw	272.26	497.60	529.20	524.01
cryst syst	orthorhombic	triclinic	monoclinic	triclinic
a (Å)	6.563(3)	9.342(4)	7.559(2)	7.498(3)
b (Å)	12.744(5)	9.889(4)	23.739(6)	10.649(4)
c (Å)	15.905(6)	10.512(4)	10.426(3)	13.673(5)
α (deg)	90	68.978(6)	90	98.602(5)
β (deg)	90	78.217(6)	108.071(4)	100.004(5)
γ (deg)	90	81.851(7)	90	110.232(5)
V (Å^3)	1330.3(9)	884.8(6)	1778.7(8)	982.5(6)
space group	*Pbcn*	$P\bar{1}$	$P2_1/n$	$P\bar{1}$
Z	4	2	4	2
ρ_{calcd} (g/cm^3)	1.359	1.868	1.976	1.771
μ(Mo Kα) (mm^{-1})	0.090	1.334	1.317	1.088
temp (K)	298(2)	293(2)	293(2)	293(2)
no. of observations ($I > 3\sigma$)	6400	3208	3867	3760
Final *R* indices [$I > 2\sigma I$] *R* and R_w[a]	0.0329, 0.0866	0.0512, 0.1379	0.0740, 0.1760	0.0590, 0.1527

[a] $R = \sum||F_o| - |F_c||/\sum|F_o|$; $R_w = \{\sum[w(F_o^2 - F_c^2)^2]/\sum[w(F_o^2)^2]\}^{1/2}$.

(vs), 1084 (vs), 858 (m), 746 (w), 672 (w), 626 (m), 551 (m) cm^{-1}. Anal. Calcd for $C_{16}H_{10}AgClN_4O_6$ (**1**): C, 38.59; H, 2.01; N, 11.25. Found: C, 38.41; H, 2.21; N, 11.17. UV−vis spectrum (in CH_3CN at room temperature): λ_{max} 297 nm.

Preparation of $\{[Ag(L7)]SO_3CF_3\}_n$ (2). A solution of $AgSO_3CF_3$ (12 mg, 0.047 mmol) in benzene (10 mL) was layered onto a solution of L7 (9.0 mg, 0.033 mmol) in CH_2Cl_2 (10 mL). The solutions were left at room temperature for about 2 days, and colorless crystals were obtained. Yield: 63%. IR (KBr): 3421 (br), 2231 (s), 1621 (s), 1542 (s), 1489 (s), 1401 (m), 1265 (vs), 1176 (s), 1037 (s), 856 (m), 835 (m), 742 (m), 644 (s), 547 (s), 516 (m) cm^{-1}. Anal. Calcd for $C_{17}H_8AgF_3N_4O_4S$ (2): C, 38.55; H, 1.51; N, 10.58. Found: C, 38.39; H, 1.48; N, 10.23. UV−vis spectrum (in CH_3CN at room temperature): λ_{max} 297 nm.

Preparation of $\{[Ag(L8)]BF_4 \cdot 0.5(C_6H_6) \cdot H_2O\}_n$(3). A solution of $AgBF_4$ (10 mg, 0.051 mmol) in benzene (10 mL) was layered onto a solution of **L8** (9.0 mg, 0.033 mmol) in CH_2Cl_2 (10 mL). The solutions were left at room temperature for about 3 days, and pink crystals were obtained. Yield: 62%. IR (KBr): 3444 (br), 2235 (s), 1648 (s), 1543 (s), 1522 (m), 1490 (s), 1401 (s), 1082 (s), 1032 (s), 807 (m), 738 (m), 676 (s) cm^{-1}. Anal. Calcd for $C_{19}H_{13}AgBF_4N_4O_2$ (**3**): C, 43.51; H, 2.48; N, 10.69. Found: C, 43.32; H, 2.28; N, 10.53. UV−vis spectrum (in CH_3CN at room temperature): λ_{max} 234 nm, 279 nm.

Preparation of $\{[Ag(L8)SbF_6] \cdot H_2O\}_n$ (4). A solution of $AgSbF_6$ (17 mg, 0.049 mmol) in benzene (10 mL) was layered onto a solution of **L8** (9.0 mg, 0.033 mmol) in CH_2Cl_2 (10 mL). The solutions were left at room temperature for about 4 days, and colorless crystals were obtained. Yield: 50%. IR (KBr): 3416 (br), 2235 (m), 1619 (s), 1550 (s), 1485 (s), 1402 (s), 1292 (s), 1167 (m), 1091 (m), 915 (m), 809 (m), 741 (s), 632 (m), 477 (s) cm^{-1}. Anal. Calcd for $C_{16}H_{10}AgF_6N_4O_2Sb$ (**4**): C, 30.29; H, 1.58; N, 8.83. Found: C, 30.17; H, 1.48; N, 8.59. UV−vis spectrum (in CH_3CN at room temperature): λ_{max} 233 nm, 278 nm.

Preparation of $\{[Ag_2(L8)_2(SO_3CF_3)] \cdot H_2O\}_n$ (5). A solution of $AgSO_3CF_3$ (12 mg, 0.047 mmol) in benzene (10 mL) was layered onto a solution of **L8** (9.0 mg, 0.033 mmol) in CH_2Cl_2 (10 mL). The solutions were left at room temperature for about 2 days, and red crystals were obtained. Yield: 64%. IR (KBr): 3421 (br), 2248 (s), 1611 (s), 1550 (s), 1474 (m), 1401 (s), 1260 (vs), 1156 (s), 1029 (s), 915 (s), 809 (s), 739 (m), 682 (s), 571 (m), 517 (m) cm^{-1}. Anal. Calcd for $C_{34}H_{18}Ag_2F_6N_8O_9S_2$ (**5**): C, 37.90; H, 1.67; N, 10.40. Found: C, 37.79; H, 1.45; N, 10.47. UV−vis spectrum (in CH_3CN at room temperature): λ_{max} 233 nm, 277 nm.

Preparation of $\{[Ag_2(L8)(C_6H_6)(ClO_4)] \cdot ClO_4\}_n$ (6). A solution of $AgClO_4$ (12 mg, 0.052 mmol) in benzene (10 mL) was layered onto a solution of **L8** (9.0 mg, 0.033 mmol) in CH_2Cl_2 (10 mL). The solutions were left at room temperature for about 2 days, and colorless crystals were obtained. Yield: 61%. IR (KBr): 3449 (br), 2234 (s), 1613 (m), 1549 (s), 1487 (s), 1410 (m), 1297 (m), 1144 (vs), 1114 (vs), 1084 (vs), 915 (m), 807 (m), 736 (s), 679 (s), 628 (m), 582 (m), 455 (m) cm^{-1}. Anal. Calcd for $C_{22}H_{14}Ag_2Cl_2N_4O_9$ (**5**): C, 34.51; H, 1.83; N, 7.32. Found: C, 34.43; H, 1.68; N, 7.55. UV−vis spectrum (in CH_3CN at room temperature): λ_{max} 233 nm, 279 nm.

Preparation of $\{[Ag_2(L8)(H_2PO_4)_2]\}_n$ (7). A solution of AgH_2PO_4 (0.047 mmol) in benzene (10 mL) was layered onto a solution of **L8** (9.0 mg, 0.033 mmol) in CH_2Cl_2 (10 mL). The solutions were left at room temperature for about 4 days, and red crystals were obtained. Yield: 34%. IR (KBr): 3442 (br), 3075 (s), 2923 (m), 2233 (s), 1611 (s), 1548 (s), 1487 (s), 1407 (s), 1297 (s), 1143 (s), 1081 (s), 983 (s), 915 (s), 832 (m), 804 (s), 736 (s), 678 (s), 582 (m), 507 (m), 454 (m) cm^{-1}. Anal. Calcd for $C_{16}H_{12}Ag_2N_4O_9P_2$ (**7**): C, 28.15; H, 1.76; N, 8.21. Found: C, 27.98; H, 1.67; N, 8.16.

Single-Crystal Structure Determination. Suitable single crystals of compounds **L1** and **1**−**7** were selected and mounted in air onto thin glass fibers. X-ray intensity data were measured at 150 K on a Bruker SMART APEX CCD-based diffractometer (Mo Kα radiation, $\lambda = 0.71073$ Å). The raw frame data for **L1** and **1**−**7** were integrated into SHELX format reflection files and corrected for Lorentz and polarization effects using SAINT.[10] Corrections for incident and diffracted beam absorption effects were applied using SADABS.[10] None of the crystals showed evidence of crystal decay during data collection. All structures were solved by a combination of direct methods and difference Fourier syntheses and refined against F^2 by the full-matrix least-squares technique. Crystal data, data collection parameters, and refinement statistics for **L7** and **1**−**7** are listed in Tables 1−2. Relevant interatomic bond distances and bond angles for **1**−**7** are given in Tables 3−9.

Results and Discussion

Synthesis and Structural Analysis of Ligands L7−L8. **L7** and **L8** were synthesized by classical Sandmeyer reaction in a relatively low yield. They can be considered to be new members of the five-membered heterocycle-bridging organic

(10) Bruker Analytical X-ray Systems, Inc.: Madison, WI, 1998.

Table 2. Crystallographic Data for **4**−**7**

	4	**5**	**6**	**7**
empirical formula	$C_{16}H_{10}AgF_6N_4O_2Sb$	$C_{34}H_{18}Ag_2F_6N_8O_9S_2$	$C_{22}H_{14}Ag_2Cl_2N_4O_9$	$C_{16}H_{12}Ag_2N_4O_9P_2$
fw	633.90	1076.42	765.01	681.98
cryst syst	triclinic	triclinic	monoclinic	triclinic
a (Å)	8.2621(9)	10.713(4)	6.9681(17)	7.956(2)
b (Å)	10.6127(12)	13.449(5)	20.627(5)	9.938(3)
c (Å)	13.3685(15)	15.423(5)	17.437(4)	14.242(4)
α (deg)	98.012(2)	65.908(5)	90	106.191(4)
β (deg)	106.259(2)	74.231(5)	95.880(4)	97.322(4)
γ (deg)	112.362(2)	83.255(5)	90	107.392(4)
V (Å^3)	999.97(19)	1952.2(12)	2493.1(11)	1004.3(5)
space group	$P\bar{1}$	$P\bar{1}$	$P2_1/n$	$P2_1/n$
Z	2	2	4	2
ρ_{calcd} (g/cm^3)	2.105	1.831	2.308	2.255
μ(Mo Kα) (mm^{-1})	2.405	1.203	1.846	2.171
temp (K)	298(2)	293(2)	293(2)	293(2)
no. of observations ($I > 3\sigma$)	3637	7113	4630	3482
final *R* indices [$I > 2\sigma I$] *R* and R_w[a]	0.0478, 0.1254	0.0540, 0.1270	0.0646, 0.1183	0.0775, 0.1648

[a] $R = \sum||F_o| - |F_c||/\sum|F_o|$; $R_w = \{\sum[w(F_o^2 - F_c^2)^2]/\sum[w(F_o^2)^2]\}^{1/2}$.

Table 3. Interatomic Distances (Å) and Bond Angles (deg) for **1**[a]

Ag(1)−N(3)#1	2.261(4)	Ag(1)−N(1)#2	2.320(4)
Ag(1)−N(2)	2.329(4)	Ag(1)−O(6)	2.458(5)
N(3)#1−Ag(1)−N(1)#2	112.11(15)	N(3)#1−Ag(1)−N(2)	114.51(15)
N(1)#2−Ag(1)−N(2)	127.88(12)	N(3)#1−Ag(1)−O(6)	120.4(2)
N(1)#2−Ag(1)−O(6)	91.31(18)	N(2)−Ag(1)−O(6)	84.62(18)
N(2)−N(1)−Ag(1)#2	119.7(2)	C(8)−N(1)−Ag(1)#2	133.6(3)

[a] Symmetry transformations used to generate equivalent atoms: #1 $x + 1, y - 1, z$; #2 $-x + 1, -y, -z + 1$; #3 $x - 1, y + 1, z$.

Table 4. Interatomic Distances (Å) and Bond Angles (deg) for **2**[a]

Ag(1)−N(2)#1	2.319(5)	Ag(1)−N(3)	2.333(5)
Ag(1)−N(4)#2	2.380(6)	Ag(1)−O(2)	2.523(6)
N(2)#1−Ag(1)−N(3)	128.06(16)	N(2)#1−Ag(1)−N(4)#2	116.85(19)
N(3)−Ag(1)−N(4)#2	112.60(19)	N(2)#1−Ag(1)−O(2)	107.9(2)
N(3)−Ag(1)−O(2)	90.7(2)	N(4)#2−Ag(1)−O(2)	85.3(2)
N(2)−N(3)−Ag(1)	116.8(3)	C(4)−N(4)−Ag(1)#3	168.3(5)

[a] Symmetry transformations used to generate equivalent atoms: #1 $-x + 2, -y + 2, -z + 1$; #2 $x + 1/2, -y + 3/2, z + 1/2$; #3 $x - 1/2, -y + 3/2, z - 1/2$.

Table 5. Interatomic Distances (Å) and Bond Angles (deg) for **3**[a]

Ag(1)−N(3)	2.256(4)	Ag(1)−N(2)#1	2.263(4)
Ag(1)−N(4)#2	2.394(6)	Ag(1)−N(1)#3	2.433(6)
N(1)−Ag(1)#4	2.433(6)		
N(3)−Ag(1)−N(2)#1	123.85(15)	N(3)−Ag(1)−N(4)#2	119.84(18)
N(2)#1−Ag(1)−N(4)#2	100.42(17)	N(3)−Ag(1)−N(1)#3	99.12(18)
N(2)#1−Ag(1)−N(1)#3	120.71(19)	N(4)#2−Ag(1)−N(1)#3	88.6(2)
N(3)−N(2)−Ag(1)#1	117.7(3)	N(2)−N(3)−Ag(1)	118.4(3)

[a] Symmetry transformations used to generate equivalent atoms: #1 $-x + 1, -y + 1, -z + 1$; #2 $-x + 1, -y, -z + 1$; #3 $x - 1, y - 1, z$; #4 $x + 1, y + 1, z$; #5 $-x + 2, -y + 1, -z + 1$.

Table 6. Interatomic Distances (Å) and Bond Angles (deg) for **4**[a]

Ag(1)−N(2)	2.277(4)	Ag(1)−N(1)#1	2.299(4)
Ag(1)−N(4)#2	2.341(6)	Ag(1)−N(3)#3	2.344(6)
N(2)−Ag(1)−N(1)#1	121.21(15)	N(2)−Ag(1)−N(4)#2	117.5(2)
N(1)#1−Ag(1)−N(4)#2	103.0(2)	N(2)−Ag(1)−N(3)#3	102.5(2)
N(1)#1−Ag(1)−N(3)#3	114.0(2)	N(4)#2−Ag(1)−N(3)#3	96.2(2)

[a] Symmetry transformations used to generate equivalent atoms: #1 $-x + 2, -y + 1, -z$; #2 $-x + 1, -y, -z$; #3 $x, y - 1, z$; #4 $x, y + 1, z$.

Table 7. Interatomic Distances (Å) and Bond Angles (deg) for **5**[a]

Ag(1)−N(2)	2.275(4)	Ag(1)−N(8)#1	2.288(5)
Ag(1)−N(5)	2.328(4)	Ag(1)−N(1)#2	2.421(6)
Ag(2)−N(3)	2.240(4)	Ag(2)−N(7)#3	2.259(5)
Ag(2)−N(4)	2.293(4)	Ag(2)−N(6)#4	2.447(5)
N(2)−Ag(1)−N(8)#1	127.09(17)	N(2)−Ag(1)−N(5)	120.01(13)
N(8)#1−Ag(1)−N(5)	102.25(17)	N(2)−Ag(1)−N(1)#2	100.92(16)
N(8)#1−Ag(1)−N(1)#2	93.1(2)	N(5)−Ag(1)−N(1)#2	108.89(17)
N(3)−Ag(2)−N(7)#3	123.31(17)	N(3)−Ag(2)−N(4)	120.91(14)
N(7)#3−Ag(2)−N(4)	108.57(16)	N(3)−Ag(2)−N(6)#4	96.53(16)
N(7)#3−Ag(2)−N(6)#4	96.46(19)	N(4)−Ag(2)−N(6)#4	104.27(17)

[a] Symmetry transformations used to generate equivalent atoms: #1 $-x + 1, -y, -z + 1$; #2 $x + 1, y, z$; #3 $x - 1, y, z$; #4 $-x, -y, -z$.

Table 8. Interatomic Distances (Å) and Bond Angles (deg) for **6**[a]

Ag(1)−N(3)#1	2.193(7)	Ag(1)−N(2)	2.280(6)
Ag(2)−N(4)#2	2.303(7)	Ag(2)−N(1)	2.348(6)
Ag(2)−C(17)	2.562(8)	Ag(2)−C(18)	2.646(9)
N(3)#1−Ag(1)−N(2)	146.0(2)	N(4)#2−Ag(2)−N(1)	119.5(3)
N(4)#2−Ag(2)−C(17)	106.6(3)	N(1)−Ag(2)−C(17)	98.2(3)
N(4)#2−Ag(2)−C(18)	102.9(3)	N(1)−Ag(2)−C(18)	123.3(3)
C(17)−Ag(2)−C(18)	30.3(3)	N(1)−N(2)−Ag(1)	117.8(4)

[a] Symmetry transformations used to generate equivalent atoms: #1 $-x + 1/2, y + 1/2, -z + 3/2$; #2 $-x + 1/2, y - 1/2, -z + 3/2$.

ligands. Their structures have been fully characterized by infrared spectroscopy, elemental analysis, and ^{1}H NMR. The solid molecular structure of **L7** was determined using single-crystal X-ray diffraction to further confirm the structure of the new ligands. As shown in Figure 1, the ligand is a bent shape, which is similar to the shape of the known organic ligands **L1**−**L6**. Two terminal benzonitrile groups and the bridging oxadiazole moiety lie in the same plane and are linked together at the para position by the five-membered oxadiazole ring. The separation between the two terminal N donors is 14.76 Å, which is longer than the corresponding distances found in **L1** (10.21 Å) and **L3** (12.21 Å). **L7** and **L8** are soluble in common polar organic solvents, such as CH_2Cl_2, $CHCl_3$, THF, CH_3OH, and C_2H_5OH, which facilitates the solution reaction between the ligands and inorganic metal salts. In addition, they give us the ability to modify **L7** and **L8** to new organic spacers with different coordination functional groups by some functional group transformation reactions related to −CN.

Table 9. Interatomic Distances (Å) and Bond Angles (deg) for **7**[a]

Ag(1)−N(4)	2.277(10)	Ag(1)−N(3)#1	2.284(10)
Ag(1)−O(9)	2.371(8)	Ag(1)−O(9)#2	2.472(8)
Ag(2)−N(2)#1	2.253(7)	Ag(2)−N(1)	2.265(7)
Ag(2)−O(2)	2.407(12)	Ag(2)−O(6)#3	2.464(9)
Ag(2)−Ag(2)#1	3.356(2)		
N(4)−Ag(1)−N(3)#1	109.2(4)	N(4)−Ag(1)−O(9)	141.2(3)
N(3)#1−Ag(1)−O(9)	100.5(3)	N(4)−Ag(1)−O(9)#2	100.5(3)
N(3)#1−Ag(1)−O(9)#2	130.8(3)	O(9)−Ag(1)−O(9)#2	76.8(3)
N(2)#1−Ag(2)−N(1)	128.5(3)	N(2)#1−Ag(2)−O(2)	115.0(4)
N(1)−Ag(2)−O(2)	106.6(4)	N(2)#1−Ag(2)−O(6)#3	107.9(3)
N(1)−Ag(2)−O(6)#3	105.5(3)	O(2)−Ag(2)−O(6)#3	83.6(4)
N(2)#1−Ag(2)−Ag(2)#1	64.01(19)	N(1)−Ag(2)−Ag(2)#1	64.60(19)
O(2)−Ag(2)−Ag(2)#1	141.8(4)	O(6)#3−Ag(2)−Ag(2)#1	134.4(3)

[a] Symmetry transformations used to generate equivalent atoms: #1 $-x+1, -y+2, -z+2$; #2 $-x+2, -y+1, -z+1$; #3 $-x+1, -y+1, -z+1$.

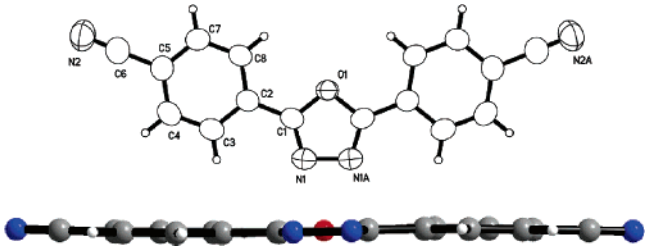

Figure 1. Molecular structure of **L7**.

Structural Analysis of $\{[Ag(L7)(H_2O)]ClO_4\}_n$ (1). Crystallization of **L7** with $AgClO_4$ in a CH_2Cl_2/C_6H_6 mixed-solvent system at room temperature produced the infinite one-dimensional chain structure in a 54% yield. Single-crystal analysis revealed that there is one kind of crystallographic Ag(I) center in **1**. Compound **1** is air stable, and the TGA trace shows that the framework of **1** is stable up to 285 °C. As shown in Figure 2, it has a distorted tetrahedral coordination sphere consisting of two $N_{oxadiazole}$ ($d_{Ag(1)-N(1)} = 2.320(4)$ Å and $d_{Ag(1)-N(2)} = 2.329(4)$ Å), one $N_{benzonitrile}$ ($d_{Ag(1)-N(3)} = 2.261(4)$ Å) from three **L7** ligands, and one O donor ($d_{Ag(1)-O(6)} = 2.458(5)$ Å) from a coordinated water molecule. It is worthwhile to point out that only one terminal −CN group on **L7** involves the Ag(I) coordination sphere. Thus, ligand **L7** acts as a tridentate ligand toward the Ag(I) ion herein. All of the Ag−N bond distances found in **1** are within the normal range for a N-containing heterocyclic Ag(I) complexes.[9] Two Ag(1) atoms are bridged by four $N_{oxadiazole}$ atoms into a $\{Ag_2N_4\}$ dinuclear core with a short Ag···Ag contact of 3.45 Å, which is identical to the sum of the van der Waals radii of two silver atoms (3.44 Å). In **1**, the ligand itself is not planar, and the three rings are slightly twisted. The uncoordinated ClO_4^- counterion is located near the Ag(I) center and hydrogen bonded to the coordinated water molecule through an O−H···O bonding interaction ($d_{O\cdots H} = 2.26(2)$ Å, $d_{O\cdots O} = 2.942(11)$ Å, and $\angle O-H\cdots O = 140(3)°$).

In the solid state, the $\{Ag_2(\mathbf{L7})_2\}$ dinuclear moieties are linked together in a hand-in-hand fashion through one of two terminal benzonitrile groups on **L7** to form a one-dimensional chain (Figure 3). In addition, hydrogen-bonding interactions are present in **1**. The one-dimensional polymer chains of **1** are linked into a two-dimensional sheet containing a square-like cavity via interchain hydrogen-bonding interactions. The weak hydrogen bonding system involves N(4) of the uncoordinated −CN group and H(4) on the **L7** ligand of the neighboring chain (Figure 3). The corresponding N···H and N···C distances are 2.52(4) and 3.36(4) Å, respectively. The uncoordinated guest water molecules are located in the square-like cavities. The existence and structural importance of the weak C−H···X hydrogen bonding interactions are now well-established[11] and are observed in many compounds, such as the N···H−C interaction in 1,3,5-tricyanobenzene-hexamethylbenzene.[12] These hydrogen bonds, although weak, contribute significantly to the alignment of the molecules of **1** in the crystalline state.

Structural Analysis of $\{[Ag(L7)]SO_3CF_3\}_n$ (2). The more strongly coordinated $SO_3CF_3^-$ anion was used instead of the more weakly coordinated ClO_4^- anion to investigate the effect of the counterion on the long range order of the Ag(1)−**L7** coordination polymer. Crystallization of **L7** with $AgClO_4$ in a CH_2Cl_2/C_6H_6 mixed-solvent system at room temperature produced the infinite noninterpenetrating three-dimensional polymeric compound **2** in a 63% yield. Compound **2** is air stable, and TGA shows that compound **2** is stable up to 275 °C. As shown in Figure 4, there is one kind

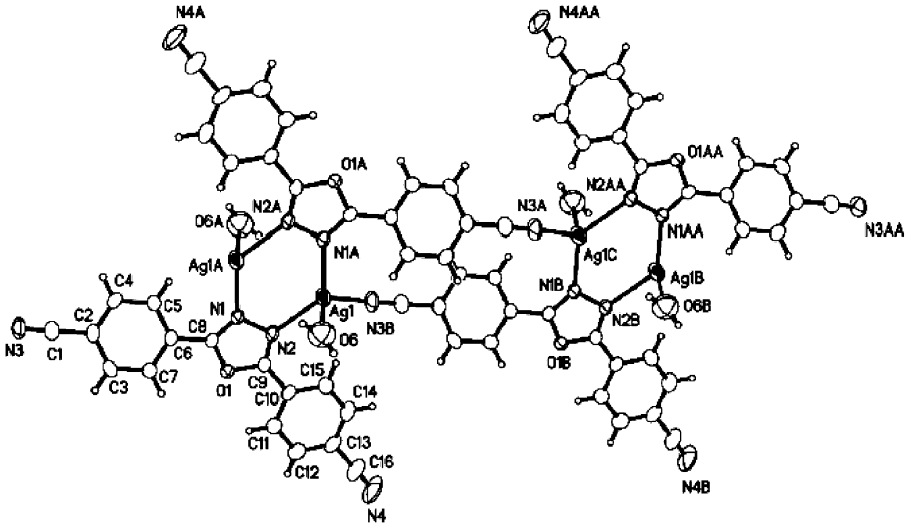

Figure 2. ORTEP figure of **1** showing the atom labeling and 50% thermal ellipsoids.

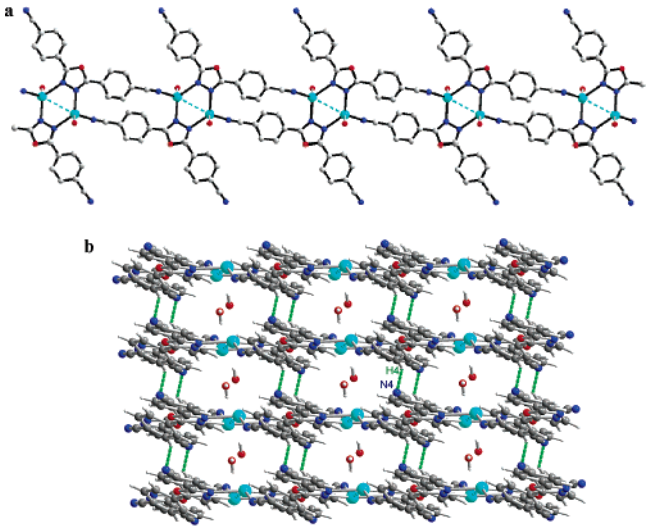

Figure 3. (a) One-dimensional chain and (b) two-dimensional H-bonded network in **1** (One set of the hydrogen bonds is labeled). Ag(I)···Ag(I) interactions and hydrogen bonds are shown as dotted lines.

of crystallographic Ag(1) center in **2**. It adopts a distorted tetrahedral coordination sphere that consists of one $O_{triflate}$, two $N_{oxadiazole}$, and one $N_{benzonitrile}$ from three tridentate **L7** ligands. The corresponding Ag(I)−$O_{triflate}$, Ag(I)−$N_{oxadiazole}$, and Ag(I)−$N_{benzonitrile}$ bonding distances are 2.523(6), 2.333(5), 2.380(6), and 2.319(5) Å, respectively. The Ag(I) and **L7** connectivity has −Ag−N−N−Ag−N−N− groupings, which are the same as those observed in compound **1**. The Ag···Ag distance (3.44 Å) is the same as the sum of the van der Waals radii of two silver atoms. The $Ag_2(\mathbf{L7})_2$ unit is introduced into a two-dimensional net instead of one-dimensional chain, which is different from **1**. This two-dimensional net is undulating and exhibits a Chinese housetop fashion (Figure 5). Coordinated $SO_3CF_3^-$ counterions are located between the layers and, furthermore, link the two-dimensional layers into a three-dimensional network through somewhat long Ag(I)−$O_{triflate}$ bonds (Figure 5).

The common feature of compounds **1** and **2** is the possession of a $\{Ag_2(\mathbf{L7})_2\}$ molecular sub-building block. In compounds **1** and **2**, **L7** exhibits similar coordination behavior (i.e., uses only one of the two terminal −CN coordination sites to bind the Ag(1) atom). Although different metal-to-ligand ratios were tried, compounds **1** and **2** were the only products isolated. different templating effects and coordination behaviors from the counterions might explain why compounds **1** and **2** pass from a one-dimensional chain to a three-dimensional framework.

Structural Analysis of $\{[Ag(L8)]BF_4 \cdot 0.5(C_6H_6) \cdot H_2O\}_n$ (3). The reason that ligand **L8** was used was to control the supramolecular motifs through 3,3′-bibenzonitrile-type ligands. It is well-known that the relative orientations of the nitrogen donors and the different bridging space may result in unusual building blocks, which can lead to the construction of supramolecular motifs that have not been achieved using normal rigid linear organic ligands. Our previous studies demonstrated that the five-membered 1,3,4-oxadiazole-bridged 3,3′-bipyridine and 3,3′-biphenylamine ligands could bind metal ions with a cis or trans conformation and result in a versatile framework topology, sometimes even affecting the formation of the polymer versus the molecule.[9]

The **L8** ligand reacted with $AgBF_4$ in CH_2Cl_2/C_6H_6 at room temperature to produce the polymeric compound **3** as pink crystals with a novel noninterpenetrating three-dimensional network in a 62% yield. Thermogravimetric analysis shows that the benzene guest molecules are lost at 170−190 °C and that the framework is stable up to ∼270 °C. As shown in Figure 6, the Ag(I) center lies in a distorted tetrahedral coordination sphere which consists of two $N_{oxadiazole}$ and two $N_{benzonitrile}$ donors from four **L8** ligands. The Ag−$N_{benzonitrile}$ and Ag−$N_{oxadiazole}$ bond distances range from 2.394(6) to 2.433(6) Å and from 2.256(4) to 2.263(4) Å, respectively. It is worth pointing out that the coordination behavior of **L8** is different from that of **L7** in **1** and **2**. The ligand **L8** herein acts as a tetradentate spacer instead of a tridentate spacer toward the Ag(1) ion. An $\{Ag_2N_4\}$ six-membered ring the same as that found in compounds **1** and **2** has been found in **3**. The corresponding Ag···Ag contact is 3.52(4) Å, which is slightly longer that those of **1** and **2**. Four $\{Ag_2N_4\}$ units are connected by tetradentate **L8** ligands to form a molecular cage in which a guest benzene molecule is located and fixed by the $\pi-\pi$ interactions between

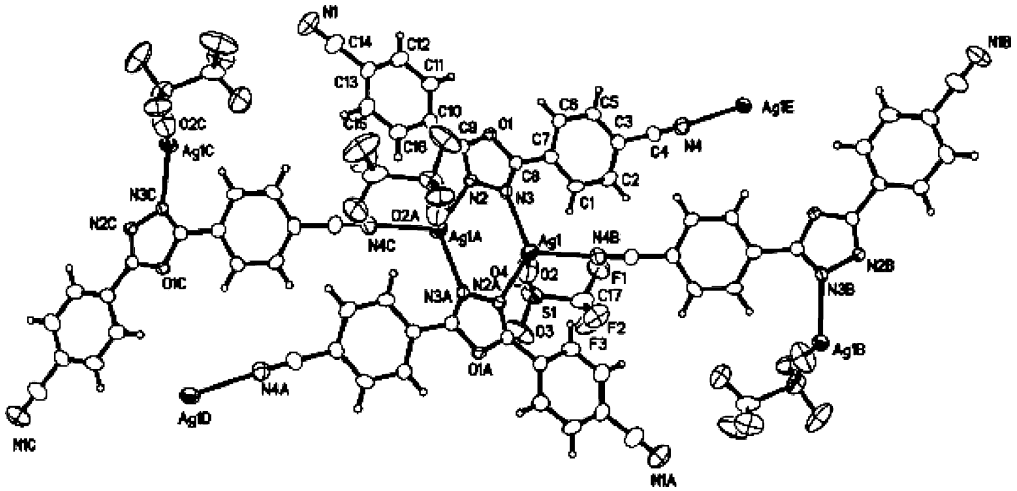

Figure 4. ORTEP figure of **2** showing the atom labeling and 50% thermal ellipsoids.

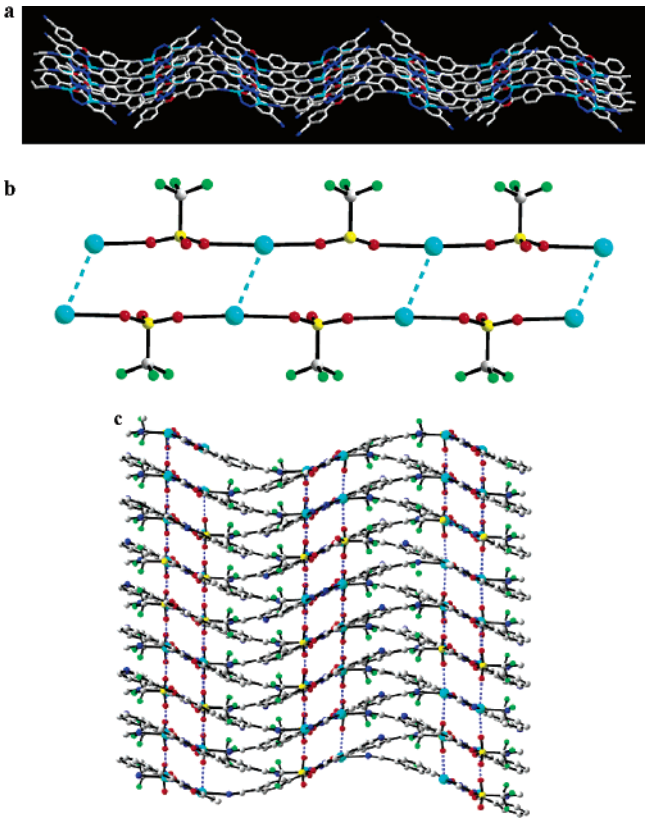

Figure 5. (a) Single two-dimensional wavelike network, (b) triflate−Ag(I) linkage, and (c) three-dimensional framework in **2**.

oxadiazole and benzene (Figure 7).[13] The longest and shortest Ag···Ag distances in the cage are 7.5 and 16.5 Å. The accessible void volume of the channels in one unit cell is 122.1 $Å^3$, which is estimated to be 12.4% of the total volume (982.5 $Å^3$).

In the solid state, compound **3** exhibits a novel noninterpenetrating cationic two-dimensional network which is parallel to the crystallographic *ab* plane. The crystal packing of **3** is shown in Figure 8. All of the two-dimensional nets stack exactly together along the crystallographic *c* axis to generate honeycomb-like channels. Inside the channels, uncoordinated BF_4^- counterions, water, and benzene molecules stack neatly upon each other to form a guest column (Figure 8). In the column, the distance between two adjacent benzene planes is 13.67 Å. Although the hexagon represents the one of the most common motifs in nature,[14] synthetic noninterpenetrating networks with honeycomb-like cross sections are still unusual because two-dimensional nets are always inclined to stack in an −ABAB− or −ABCABC− stacking sequence, such as the stacking fashion observed in compound [Ag(TCB)(CF_3SO_3)] (TCB = 1, 3,5-tricyanobenzene);[14b,15] therefore, the assembly of honeycomb-like channels is challenging.

Structural Analysis of {[Ag(L8)SbF_6]·H_2O}$_n$ (4). Crystallization of **L8** with $AgSbF_6$ in the same mixed-solvent system at room temperature produced polymeric compound **4** as colorless crystals with a novel noninterpenetrating two-dimensional network in a 49% yield. TGA shows that the framework of **4** is stable up to ∼280 °C. Single-crystal X-ray analysis shows that the local coordination geometry of the Ag(I) center in compound **4** is similar to that of compound **3**. The Ag−N bond lengths lie in the range of 2.277(4)−2.344(6) Å, which are comparable to the corresponding bond distances in compound **3**. The same {Ag_2N_4} connectivity as that of compounds **1**−**3** has been found in **4** with an Ag···Ag contact of 3.65 Å. Single-crystal X-ray analysis revealed that compounds **3** and **4** are isostructural; however, for compounds **3**−**4**, there is an interesting change in the unit cell parameters upon the increase of the counterion size from BF_4^- to SbF_6^-. The cell volume increases as expected, but it does so in an anisotropic way. The shorter *a* axis expands, while the long *b* and *c* axes contract. In the solid state, compound **4** adopts the same noninterpenetrating two-dimensional network as that found in compound **3**. Honeycomb-like channels contain distorted SbF_6^- counterions and water molecules; however, no benzene solvent molecules have been found. The corresponding channel dimensions are almost identical with those in **3** (Figure 9).

Structural Analysis of {[Ag_2(L8)$_2$(SO_3CF_3)]·H_2O}$_n$ (5). The **L8** ligand reacted with $AgSO_3CF_3$ in the same mixed-solvent system at room temperature to produce the polymeric compound **5** as red crystals with a noninterpenetrating two-dimensional network in a 64% yield. TGA shows that the guest water molecules were lost at 120−130 °C and that the framework of **5** is stable up to ∼300 °C. The X-ray structure of **5** shows that there are two independent crystallographic Ag(I) centers in **5** and both lie in a distorted tetrahedral coordination sphere which is similar to that of

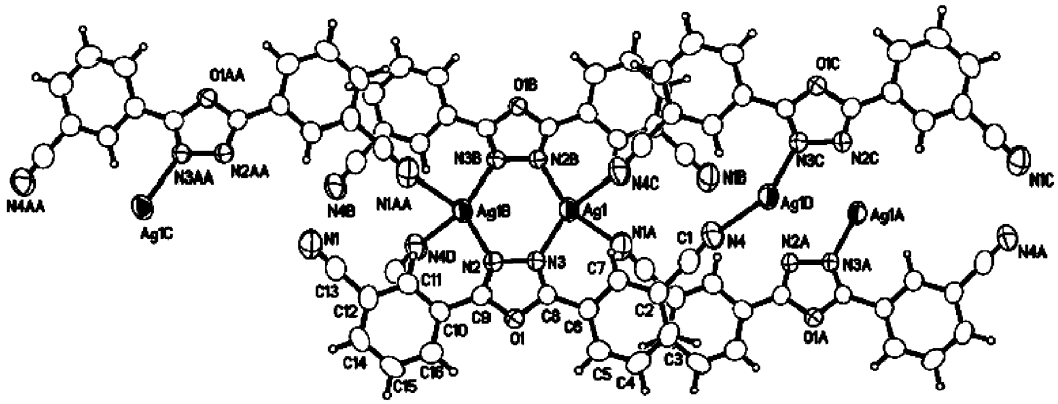

Figure 6. ORTEP figure of **3** showing the atom labeling and 50% thermal ellipsoids.

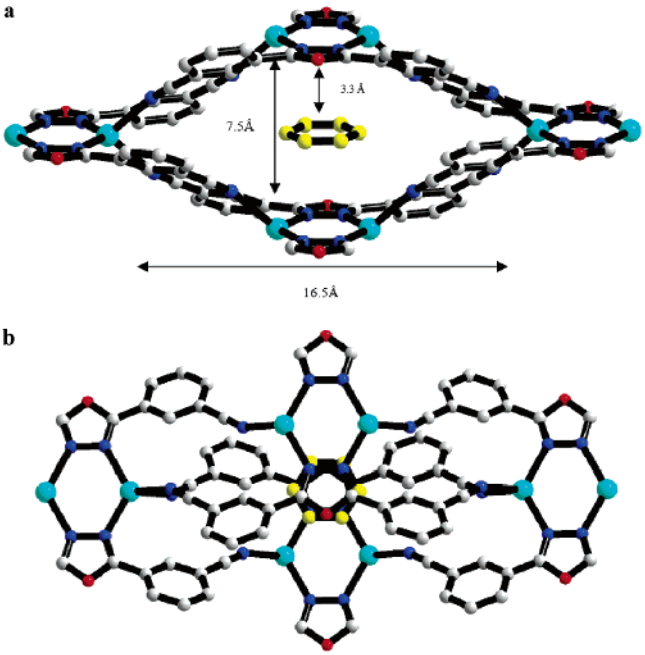

Figure 7. (a) Side and (b) top views of the molecular cage containing the benzene molecule. The benzene guest molecule is marked in yellow.

compound **3**. This distorted tetrahedral coordination environment consists of two $N_{oxadiazole}$ and two $N_{benzonitrile}$ donors from four **L8** ligands. The Ag−N bond lengths lie in the range of 2.240−2.447 Å, which are comparable to those of the corresponding bonds found in **4**. The same $\{Ag_2N_4\}$ connectivity as that in compounds **1**−**4** has been found in **5** with an Ag···Ag distance of 3.61 Å. Here, the ligand again acts as a tetradentate spacer toward these two independent Ag(I) ions. In the solid state, Ag(I) atoms are linked to each other by **L8** ligands via the $\{Ag_2N_4\}$ moiety into a noninterpenetrating honeycomb-like net, which is similar to that found in **3** and **4**. It is worthy to point out that the two-dimensional layers repeat in an −ABAB− stacking sequence instead of the stacking fashion observed in **3** and **4**. This difference may be caused by the different templating effect of the $SO_3CF_3^-$ counterion (Figure 10). In the single cage, the shortest and longest Ag···Ag distances are 8.61 and 15.82 Å, respectively.

Structural Analysis of $\{[Ag_2(L8)(C_6H_6)(ClO_4)]\cdot ClO_4\}_n$ (6). Compound **6** was obtained as colorless crystals by combination of the **L8** ligand with $AgClO_4$ in a CH_2Cl_2/C_6H_6 mixed-solvent system at room temperature in a 60% yield. The framework of **6** is stable up to ∼260 °C. The X-ray structure of **6** shows that there are two independent Ag(I) centers present the asymmetric unit (Figure 11). The

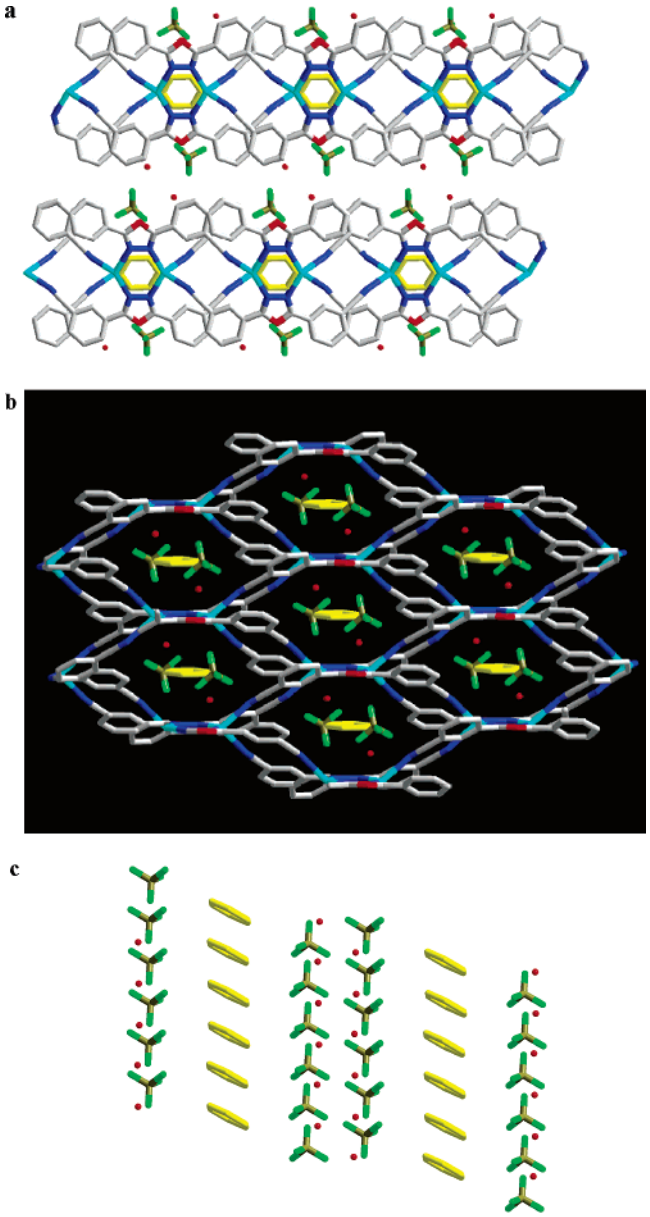

Figure 8. (a) Two sets of two-dimensional nets (view down the crystallographic *a* axis), (b) a view of **3** perpendicular to the channels, and (c) the packing diagram of the triflate anions, benzene, and water guest molecules in **3** (view down the crystallographic [110] direction).

first kind of Ag(1) atom is coordinated by one $N_{benzonitrile}$ (Ag(1)−N(3)#1 = 2.193(7) Å) and one $N_{oxadiazole}$ (Ag(1)−N(2) = 2.280(6) Å) donors from two **L8** ligands and one O donor (O(6)) from one ClO_4^- anion in the equatorial plane with the other two perchlorate O donors (Ag(1)−O(3) = 2.694(6) Å and Ag(1)−O(5) = 2.825(6) Å) in the axial positions, thus forming the distorted trigonal bipyramidal geometry of $\{AgN_2O_3\}$. The second Ag(2) center lies in a $\{AgN_2O_2\pi\}$ coordination environment which is composed of two N donors from the benzonitrile (Ag(2)−N(4)#2 = 2.303(7) Å) and oxadiazole (Ag(2)−N(1) = 2.348(6) Å) moieties of two individual **L8** ligands, two weakly coordinated O donors from a bidentate ClO_4^- counterion with somewhat long Ag−O distances at 2.819(6) and 2.795(6) Å, respectively, and a π donor from a coordinated benzene solvent molecule. The Ag(2)−C(17) and Ag(2)−C(18) bond

(11) Desiraju, G. R. *Acc. Chem. Res.* **1996**, *29*, 441.
(12) Reddy, D. S.; Goud, B. S.; Panneerselvam, K.; Desiraju, G. R. *J. Chem. Soc. Commun.* **1993**, 663.
(13) Chen, C.-L.; Su, C.-Y.; Cai, Y.-P.; Zhang, H.-X.; Xu, A.-W.; Kang, B.-S.; zur Loye, H.-C. *Inorg. Chem.* **2003**, *42*, 3738.
(14) Choi, H. J.; Suh, M. P. *J. Am. Chem. Soc.* **1998**, *120*, 10622. (b) Gardner, G. B.; Venkataraman, D.; Moore, J. S.; Lee, S. *Nature* **1995**, *374*, 792. (c) Abrahams, B. F.; Hoskins, B. F.; Liu, J.; Robson, R. *J. Am. Chem. Soc.* **1991**, *113*, 3045. (d) Abrahams, B. F.; Hoskins, B. F.; Robson, R. *J. Chem. Soc., Chem. Commun.* **1990**, 60.
(15) Pshirer, N. G.; Ciurtin, D. M.; Smith, M. D.; Bunz, U. H. F.; zur Loye, H.-C. *Angew. Chem., Int. Ed.* **2002**, *41*, 583.

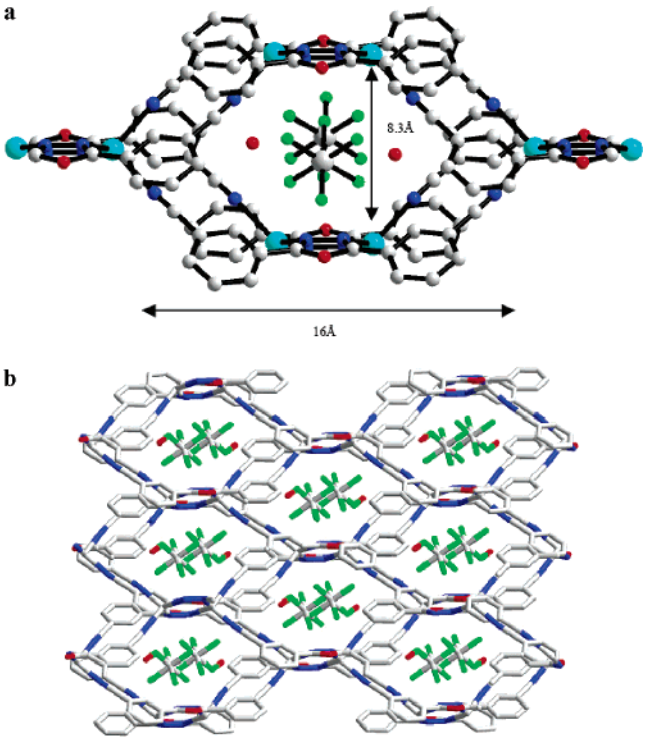

Figure 9. (a) Molecular cage and (b) two-dimensional net in **4**. No benzene guest molecules are found in the honeycomb-like channels.

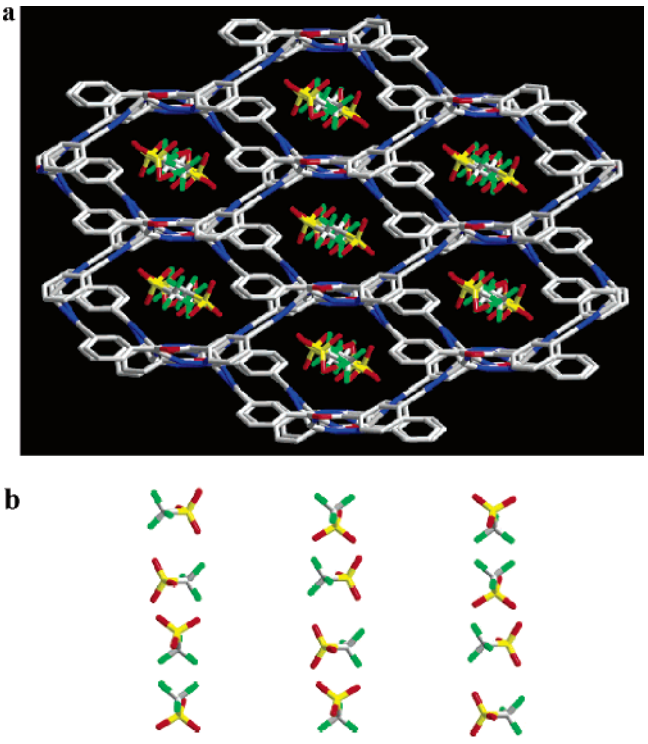

Figure 10. (a) Two-dimensional net in **5** stacking together in an −ABAB− fashion and (b) the packing diagram of the triflate anions in **5**.

distances are 2.562(8) and 2.646(9) Å, respectively, while the remaining Ag−C contact distances are greater than 2.80 Å, which is beyond the limits (2.47−2.80 Å) commonly observed in Ag(I)−aromatic complexes.[16]

(16) Griffith, E. A. H.; Amma, E. L. *J. Am. Chem. Soc.* **1974**, *96*, 5407. (b) Rodesiler, P. F.; Amma, E. L. *Inorg. Chem.* **1972**, *11*, 388.

In the solid state, Ag(1) and Ag(2) atoms are linked together by the tetradentate **L8** ligands into a undulating one-dimensional chain extended along the crystallographic *b* axis (Figure 12). It is worth pointing out that compound **6** contains the $\{Ag_2N_2O\}$ moiety instead of the $\{Ag_2N_4\}$ cluster core that is commonly observed in oxadiazole-bridging ligands−Ag(I) coordination polymers. The corresponding Ag(1)···Ag(2) distance in the $\{Ag_2N_2O\}$ moiety contact is 3.66 Å, which is slightly longer that those of **1**−**5**. As shown in Figure 13, these one-dimensional chains are connected to each other by $\{AgClO_4\}$ linkages along the crystallographic *a* axis to form a two-dimensional porous network, in which coordinated benzene molecules are located. Thermogravimetric analysis indicates that these coordinated benzene molecules are lost in the temperature range of 140−180 °C.

Structural Analysis of $\{[Ag_2(L8)(H_2PO_4)_2]\}_n$ (7). The more strongly coordinating $H_2PO_4^-$ anion was used instead of the weakly coordinating counterions to investigate the effect of the counterion on the long range order of the Ag(I)−**L8** coordination polymer. Compound **7** was synthesized by the combination of **L8** and AgH_2PO_4 in a CH_2Cl_2/C_6H_6 mixed-solvent system which produced red crystals in a 34% yield. An ORTEP drawing of **7** with the atom numbering scheme is shown in Figure 14. There are two different Ag(I) centers in **7**. They reside in a distorted tetrahedral coordination sphere. For Ag(1), its coordination environment consists of two $N_{benzonitrile}$ from two **L8** ligands and two O donors from two $H_2PO_4^-$ anions. The Ag(1)−N distances are 2.277(10) and 2.284(10) Å, while the Ag(1)−O distances are 2.371(8) and 2.472(8) Å. The Ag(2) center is connected to two $N_{oxadiazole}$ donors and two O donors from two $H_2PO_4^-$. The Ag(2)−N bond lengths are 2.265(7) and 2.253(7) Å, while the Ag(2)−O bond lengths are 2.407(12) and 2.464(9) Å. As shown in Figure 15, two **L8** ligands arrange in a face-to-face fashion to coordinate four Ag(I) ions from opposite directions, generating a tetranuclear $\{Ag_4(\mathbf{L8})_2\}$ plane, in which the shortest and longest Ag(I)···Ag(I) distances are 3.356(2) and 15.82(2) Å. Two tetranuclear planes are further linked by bidentate coordinated $H_2PO_4^-$ counterions through two Ag(1)−H_2PO_4−Ag(2) linkages into a cagelike sub-building block which is filled with two monodentrate $H_2PO_4^-$ anions. These cagelike sub-building blocks are bound together by four $\{Ag_2O_2\}$ fragments into a novel two-dimensional net extended in the crystallographic *ac* plane (Figure 16). In the net, all of the $\{Ag_4(\mathbf{L8})_2\}$ planes are exactly parallel and vertical to the two-dimensional net.

Ligand **L8** adopts a trans conformation to bind Ag(I) centers in compounds **3**−**7**, which is different than the coordination behavior of its analogues **L2**, **L4**, and **L6**. Our previous study shows that **L2**, **L4**, and **L6** could adopt either a cis or trans conformation to link the metal atoms into coordination polymers or suporamolecular complexes.[9] For example, the combination of **L2** with M(II) (M = Cu and Zn) in a CH_3CN/CH_2Cl_2 solution generated the dimeric macrocycles $[Zn(cis\text{-}\mathbf{L2})(H_2O)_3(NO_3)]_2(NO_3)_2$ and $\{[Cu(cis\text{-}\mathbf{L2})(CH_3CN)(NO_3)]_2$. Compounds **1**−**7** are insoluble in common organic solvents because of their polymeric nature. They are soluble in CH_3CN and slightly soluble in DMSO

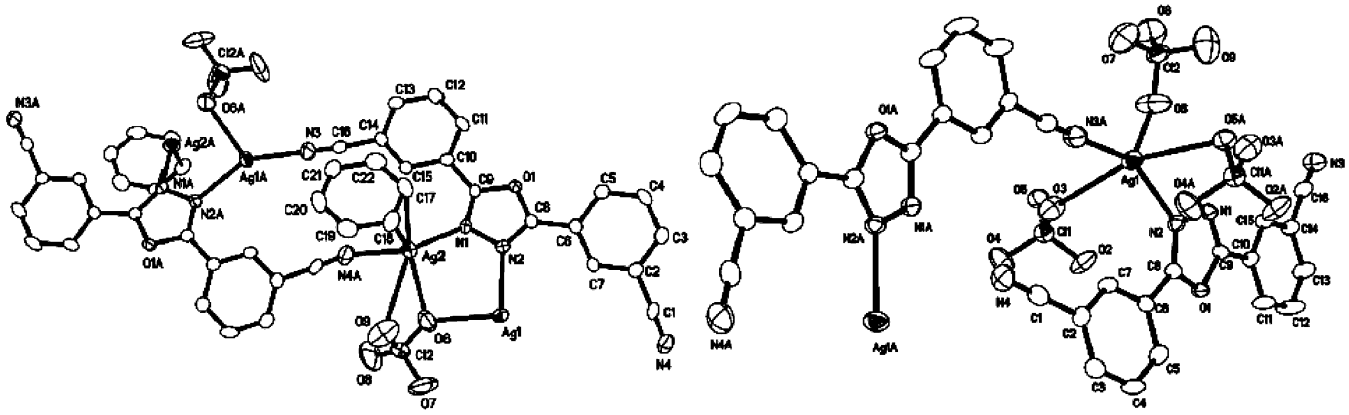

Figure 11. Ag(1) and Ag(2) coordination environments in **6** with 50% probability displacement ellipsoids.

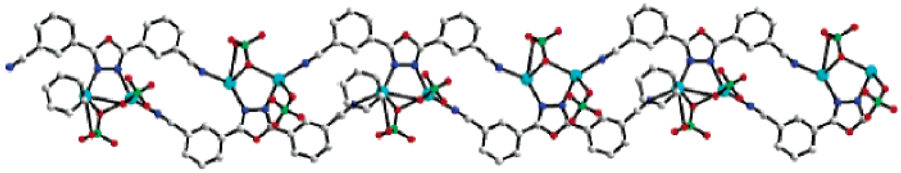

Figure 12. The undulating one-dimensional chain in **6**.

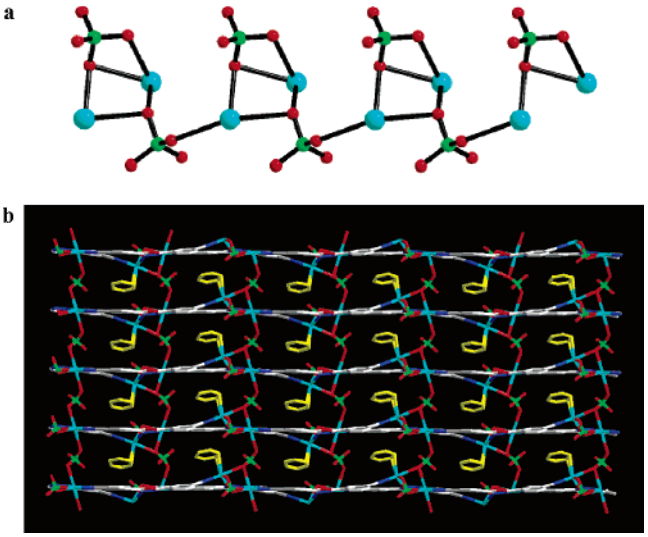

Figure 13. (a) $\{AgClO_4\}$ linkage in **6** and (b) the two-dimensional framework containing coordinated benzene molecules marked in yellow.

and DMF. In CH_3CN, all complexes were dissolved to dissociate into oligomers or the starting materials, which were identified by the UV−vis spectra (Experimental Section).

Luminescent Properties of L7 and L8 and 1−6. Inorganic−organic hybrid coordination polymers have been investigated for fluorescence properties and for potential applications as luminescent materials, such as light-emitting diodes (LEDs).[17] Because of the higher thermal stability of inorganic−organic coordination polymers and the ability to affect the emission wavelength of organic materials, syntheses of inorganic−organic coordination polymers by the judicious choice of conjugated organic spacers and transition metal centers can be an efficient method for obtaining new types of electroluminescent materials, especially for d^{10} or $d^{10}-d^{10}$ systems[18] and oxadiazole-containing complexes.[19] We have been exploring the luminescent properties of **L1**−**L6** and organic−inorganic coordination polymers and supramolecular complexes in the solid state. The results indicate that the emission colors of organic spacers **L1**−**L6** were affected by their incorporation into metal-containing coordination compounds. The luminescent properties of **L7** and **L8** and polymeric compounds **1**−**6** were investigated in CH_3CN and the solid state. The fluorescence spectra of **L7** and **L8** and **1**−**6** are summarized in Table 10. As indicated in Figure 17, in CH_3CN, **L7** and **L8** each present two maxima at 350 and 364 nm for **L7** and 342 and 347 nm for **L8**. In the solid state, **L7** and **L8** each exhibit one emission maximum at 385 and 399 nm, respectively. In the solid state, the emission colors of the free ligands were slightly affected by their incorporation into the Ag-containing polymeric compounds **1**−**6**, as evidenced by the small shift in the emission. We thus believe that the luminescence of **1**−**6** originate from ligand-centered n−π^* or $\pi-\pi^*$ process.[18g] In CH_3CN, almost no difference has been found between ligand and the complex's emission colors. This implies that the polymeric complexes disaggregate into oligomers or starting materials in acetonitrile.

(17) Ciurtin, D. M.; Pschirer, N. G.; Smith, M. D.; Bunz, U. H. F.; zur Loye, H.-C. *Chem. Mater.* **2001**, *13*, 2743. (b) Cariati, E.; Bu, X.; Ford, P. C. *Chem. Mater.* **2000**, *12*, 3385. (c) Würthner, F.; Sautter, A. *Chem. Commun.* **2000**, 445.

(18) Harvey, P. D.; Gray, H. B. *J. Am. Chem. Soc.* **1988**, *110*, 2145. (b) Catalano, V. J.; Kar, H. M.; Bennett, B. L. *Inorg. Chem.* **2000**, *39*, 121. (c) Tong, M.-L.; Chen, X.-M.; Ye, B.-H.; Ji, L.-N. *Angew. Chem., Int. Ed.* **1999**, *38*, 2237. (d) Burini, A.; Bravi, R.; Fackler, J. P., Jr.; Galassi, R.; Grant, T. A.; Omary, M. A.; Pietroni, B. R.; Staples, R. J. *Inorg. Chem.* **2000**, *39*, 3158. (e) Seward, C.; Jia, W.-L.; Wang, R.-Y.; Enright, G. D.; Wang, S.-N. *Angew. Chem., Int. Ed.* **2004**, *43*, 2933. (f) Yam, V. W.-W.; Lo, K. K.-W. *Chem. Soc. Rev.* **1999**, *28*, 323. (g) Wu, C.-D.; Ngo, H. L.; Lin, W. *Chem. Commun.* **2004**, 1588.

(19) Hu, N.-X.; Esteghamatian, M.; Xie, S.; Popovic, Z.; Hor, A.-M.; Ong, B.; Wang, S.-N. *Adv. Mater.* **1999**, *11*, 1460. (b) de Silva, A. S.; de Silva, M. A. A.; Carvalho, C. E. M.; Antunes, O. A. C.; Herrera, J. O. M.; Brinn, I. M.; Mangrich, A. S. *Inorg. Chim. Acta* **1999**, *292*, 1. (c) Wang, J.; Wang, R.; Yang, J.; Zheng, Z.; Carducci, M. D.; Cayou, T.; Peyghambarian, N.; Jabbour, G. E. *J. Am. Chem. Soc.* **2001**, *123*, 6179.

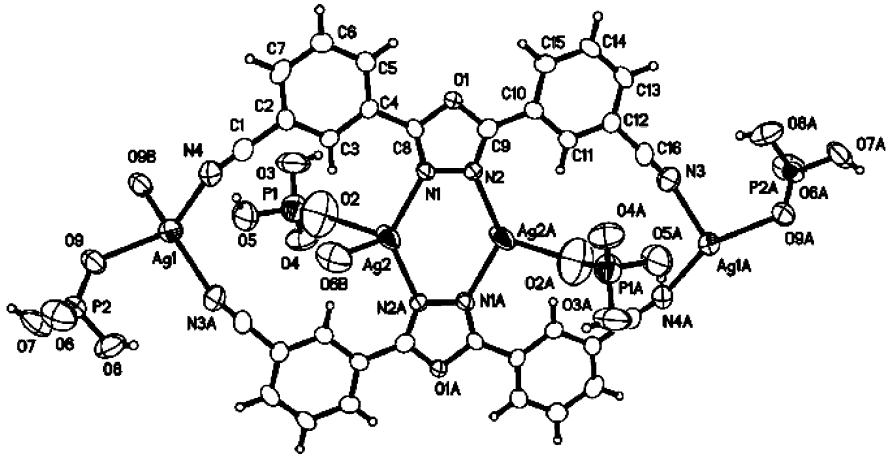

Figure 14. Ag(I) coordination environments in **7**. Displacement ellipsoids drawn at the 50% probability level.

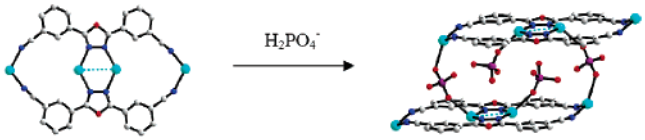

Figure 15. $\{Ag_4(\mathbf{L8})_2\}$ planar moiety linked by $H_2PO_4^-$ into cagelike sub-building block.

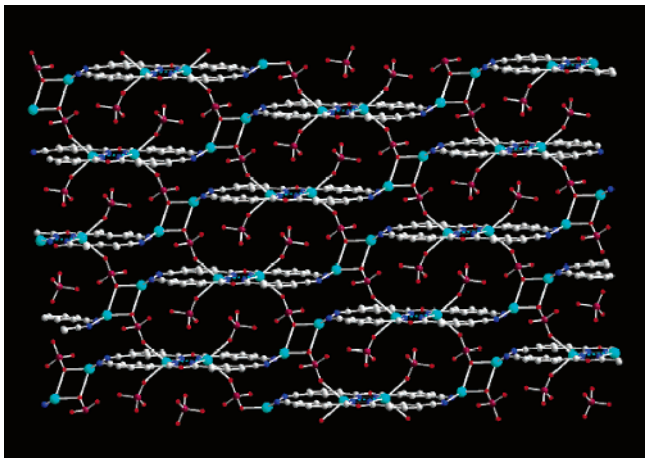

Figure 16. Perspective view of two-dimensional layer in **7**.

Host−Guest Chemistry of Compound 3. The most important factor in seeking and developing new molecular-based porous materials is that the frameworks of such materials are stable even after removal of the guest molecules.[20] As we know, many porous systems, upon removal of the included guest molecule, often undergo phase transitions to other more dense structures.[21] Primary guest sorption experiments were performed on **3** with benzene to explore the reversible adsorption and readsorption of **3** in solution. The experimental results show that **3** exhibits a clear affinity for the benzene molecule and can reversibly desorb and reabsorb this guest molecule at room temperature. The desolvated sample was prepared by heating the as-synthesized crystals of **3**. The ^{1}H NMR spectra and TGA trace show that all benzene guest molecules could be removed at ~190 °C (Figure 18). The X-ray powder diffraction (XRD) pattern of a thermally desolvated sample of **3** was compared with that of an as-synthesized solvent-containing sample of **3** in Figure 19. The XRD pattern after heating shows that the shapes and intensities of some reflections are slightly changed relative to that of the original sample. This means that guest loss does not result in symmetry change or cavity volume collapse. When the desolvated solids are immersed in benzene for 24 h at room temperature, an XRD pattern nearly identical to that obtained for the original crystals is regenerated indicating that the benzene molecules were re-

Table 10. Luminescent Properties of **L7** and **L8** and **1**−**6** in the Solid State and CH_3CN

	solid state ($\lambda_{ex}/\lambda_{em}$)	CH_3CN ($\lambda_{ex}/\lambda_{em}$)		solid state ($\lambda_{ex}/\lambda_{em}$)	CH_3CN ($\lambda_{ex}/\lambda_{em}$)
L7	224/399	296/350, 364	**3**	204/383	295/330, 345
L8	208/385	297/342, 347	**4**	206/373	298/345
1	204/386	299/348, 363	**5**	204/375	284/332, 346
2	210/393	297/349, 364	**6**	206/378, 388	296/347

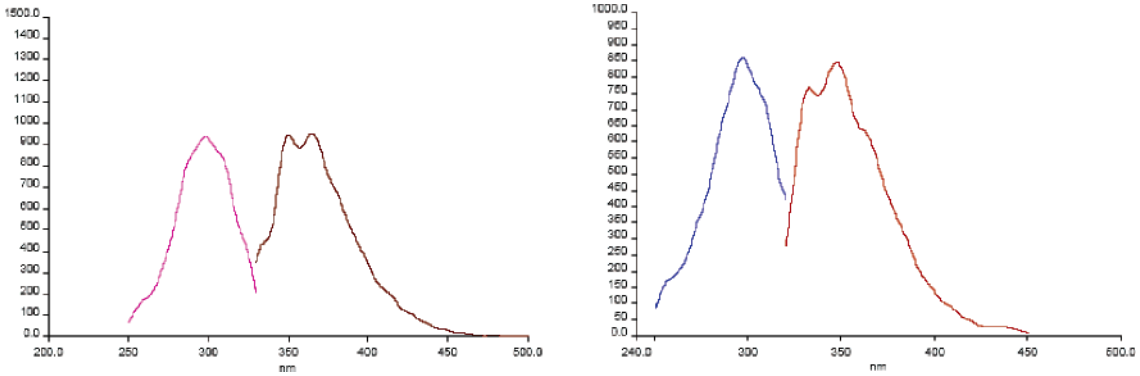

Figure 17. Photoinduced ex- and emission spectra of **L7** (left) and **L8** (right) in CH_3CN.

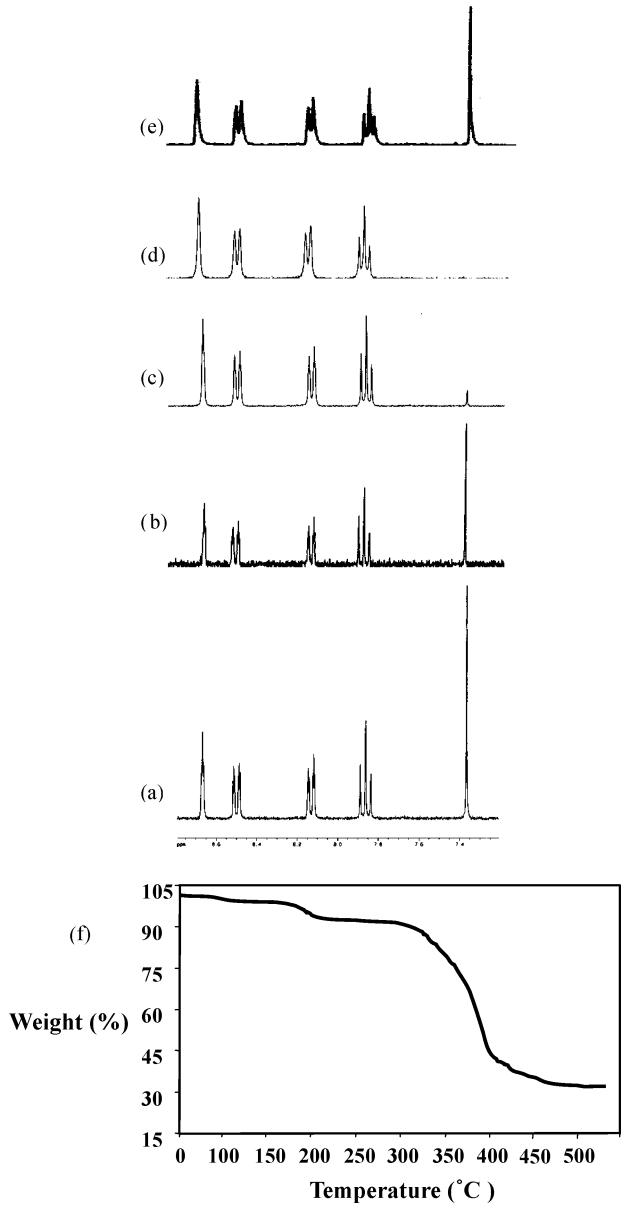

Figure 18. ^{1}H NMR spectra of **3** in DMSO-d_6. (a) ^{1}H NMR spectrum of original sample of **3** recorded at room temperature. (b) The solid sample of **3** was heated to 120 °C, then dissolved in DMSO-d_6, and the spectrum was recorded at ambient temperature. (c) The solid sample of **3** was heated to 180 °C, then dissolved in DMSO-d_6, and the spectrum was recorded at ambient temperature. (d) The solid sample of **3** was heated to 190 °C, then dissolved in DMSO-d_6, and the spectrum was recorded at ambient temperature. (e) Complex **3** immersed in benzene for 24 h and then dried at room temperature for 2 days. (f) TGA trace of compound **3**.

incorporated into the framework under these mild conditions. After the sample was taken out of the benzene, it was dried at room temperature for 48 h before recording the ^{1}H NMR. The ^{1}H NMR confirmed the re-uptake of benzene to the extent of 93%. Because **3** is insoluble in benzene, the possibility of a dissolution−recrystallization mechanism to explain the solvent reabsorption is unlikely.

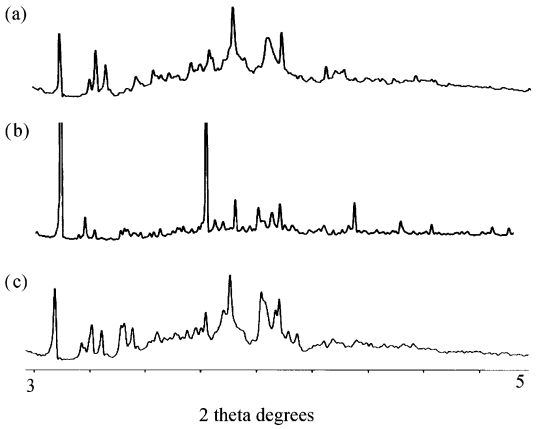

Figure 19. X-ray powder diffraction patterns of **3**. (a) The original crystals of **3**, (b) **3** heated to 190 °C and (c) sample obtained by immersing (b) in benzene for 24 h at room temperature and then dried at room temperature for 2 days.

Table 11. Electrical Conductivity of Compounds **1**−**6**

	L (μm)	G (ns)	B (μs)	r ($\times 10^{-5}\,\Omega^{-1}\,cm^{-1}$)	ρ^a ($\times 10^2\,\Omega$ m)	$\epsilon_r{}^b$ ($\times 10^2$)
1	26.33	170.76	6.03	2.87	3.48	3.64
2	128.01	128.21	5.74	10.47	0.955	16.83
3	54.41	40.01	5.76	1.39	7.19	7.17
4	61.02	174.43	6.02	6.79	1.47	8.42
5	150.08	40.94	5.33	3.92	2.55	18.30
6	47.01	168.03	6.19	5.04	1.98	6.66

[a] Resistivity (ρ) of **1**−**6** was obtained depending on the formula S/LG ($S = \pi r^2$, L = length of the single crystals). [b] Dielectric constant (ϵ_r) of **1**−**6** was obtained depending on the formula $BL/2\pi fs$.

Electrical Conductivity. Synthesis of single-component molecular coordination complexes by the judicious choice of organic spacers and metal centers can be an efficient method for obtaining new types of conductive materials,[22] for example, $[M(dimt)_2]_2$-type molecular complexes (M = Ni(II), Pd(II), Pt(II), Cu(II), and so on; dimt = 4,5-dimercapto-1,3-dithiole-2-thione).[23] Some of these complexes have been confirmed to be semiconductors or superconductors. Up to now, a number of molecular-based transition metal complexes with interesting electrical conductivity have been reported. However, the study of conductive properties on polymeric coordination complexes has received considerably less attention. The electrical conductive experiments were performed on compounds **1**−**6** in the solid state to explore the electrical conductive properties of these new polymeric complexes. The conductivity measurements of **1**−**6** were performed on single crystals at a direction on *bc* plane using an Agilent Technologies instrument (4294A-ATO-20150) with a scan range of 5(0.1) MHz. The primary result indicates that compounds **1**−**6** behave as typical semiconductors with a resistivity (ρ) value lying in the range of $9.55 \times 10-7.19 \times 10^2$ Ωm (Table 11). The dielectric

(20) Gardner, G. B.; Kiang, Y.-H.; Lee, S.; Asgaonkar, A.; Venkataraman, D. *J. Am. Chem. Soc.* **1996**, *118*, 6946. (b) Kepert, C. J.; Prior, T. J.; Rosseinsky, M. J. *J. Am. Chem. Soc.* **2000**, *122*, 5158. (c) Su, C.-Y.; Smith, M. D.; zur Loye, H.-C. *Angew. Chem., Int. Ed.* **2003**, *42*, 4085.

(21) Abrahams, B. F.; Hoskins, B. F.; Michail, D. M.; Robson, R. *Nature* **1994**, *369*, 727. (b) Wang, X.; Smard, M.; Wuest, J. D. *J. Am. Chem. Soc.* **1994**, *116*, 12119. (c) Venkataraman, D.; Lee, S.; Zhang, J.; Moore, J. S. *Nature* **1994**, *371*, 591. (d) Hoskins, B. F.; Robson, R. *J. Am. Chem. Soc.* **1990**, *112*, 1546.

(22) Kobayashi, A.; Tanaka, H.; Kobayashi, H. *J. Mater. Chem.* **2001**, *11*, 2078. (b) Zheng, S.-L.; Zhang, J.-P.; Wang, W.-T.; Chen, X.-M. *J. Am. Chem. Soc.* **2003**, *125*, 6882.

(23) Bousseau, M.; Valade, L.; Legros, J.-P.; Cassoux, P.; Garbauskas, M.; Interrante, V. *J. Am. Chem. Soc.* **1986**, *108*, 1908.

constants (ϵ_r) of **1**−**6** were obtained in the range of $3.64 \times 10^2 - 18.30 \times 10^2$.

Conclusions

This study demonstrates that the bent oxadiazole-bridging benzonitrile organic ligands, 2,5-bis(4-cyanophenyl)-1,3,4-oxadiazole (**L7**) and 2,5-bis(3-cyanophenyl)-1,3,4-oxadiazole (**L8**), are capable of coordinating metal centers with both $N_{pyridyl}$ and $N_{triazole}$ donors generating novel coordination polymers. Seven new polymeric compounds, **1**−**7**, were synthesized from solution reactions of L7 and L8 with various Ag(I) salts. The relative orientation of the nitrogen donors on the cyanophenyl groups and the five-membered oxadiazole spacing in L7 and L8 resulted in unusual building blocks leading to the construction of polymeric motifs, which have not been obtained using normal linear rigid bidentate organic ligands. We are currently extending this research by preparing new symmetric and unsymmetric oxadiazole-containing ligands of this type containing different coordination functional groups and having different orientations of the terminal coordination sites. We anticipate that this new type of organic ligand will result in a variety of new coordination polymers with novel polymeric patterns and interesting chemical and physical properties.

Acknowledgment. We are grateful for financial support from the National Natural Science Foundation of China (20371030 and 20174023), and the Shangdong Natural Science Foundation (Z2004B01).

Supporting Information Available: Crystallographic data in CIF format. This material is available free of charge via the Internet at http://pubs.acs.org.

IC050218S